Supplementary Information for

Structure and Dynamic Behavior of Rhodium Complexes Supported by Lewis Acidic Group 13 Metallatranes

James T. Moore, Nicholas E. Smith, Connie C. Lu

Department of Chemistry, University of Minnesota, 207 Pleasant Street SE, Minneapolis, Minnesota, 55455-0431

Table of Contents

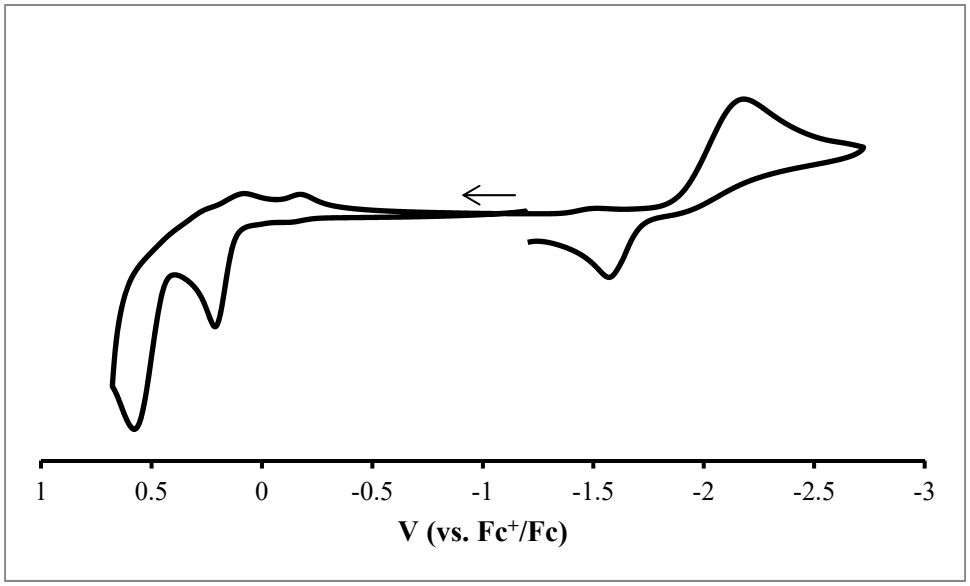

Figure S1. Full cyclic voltammogram of **1-Cl** (100 mV/s) in 0.1 M $TBAPF_6$ in THF referenced to the Fc/Fc^+ redox couple. First oxidation E_{pa} = 0.21 V; second oxidation E_{pa} = 1.00 V.

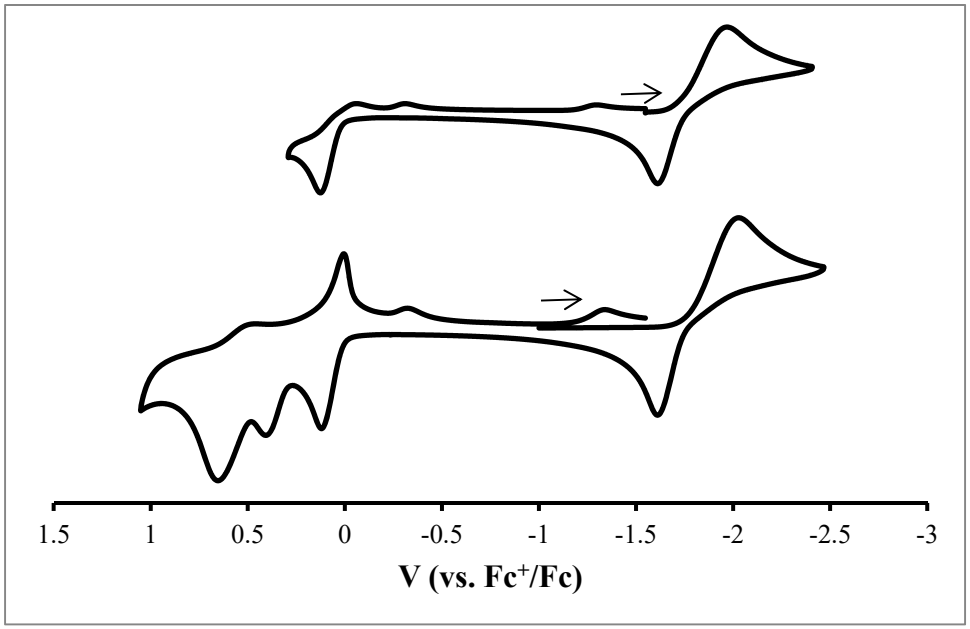

Figure S2. Cyclic voltammogram of **2-Cl** (100 mV/s) in 0.1 M $TBAPF_6$ in THF referenced to the Fc/Fc^+ redox couple. First oxidation E_{pa} = 0.12 V; second oxidation E_{pa} = 0.41 V; third oxidation E_{pa} = 0.65. The return reduction at E_{pc} = 0.81V is absent in the top CV, demonstrating that it is an electrochemical event not related to the first oxidation.

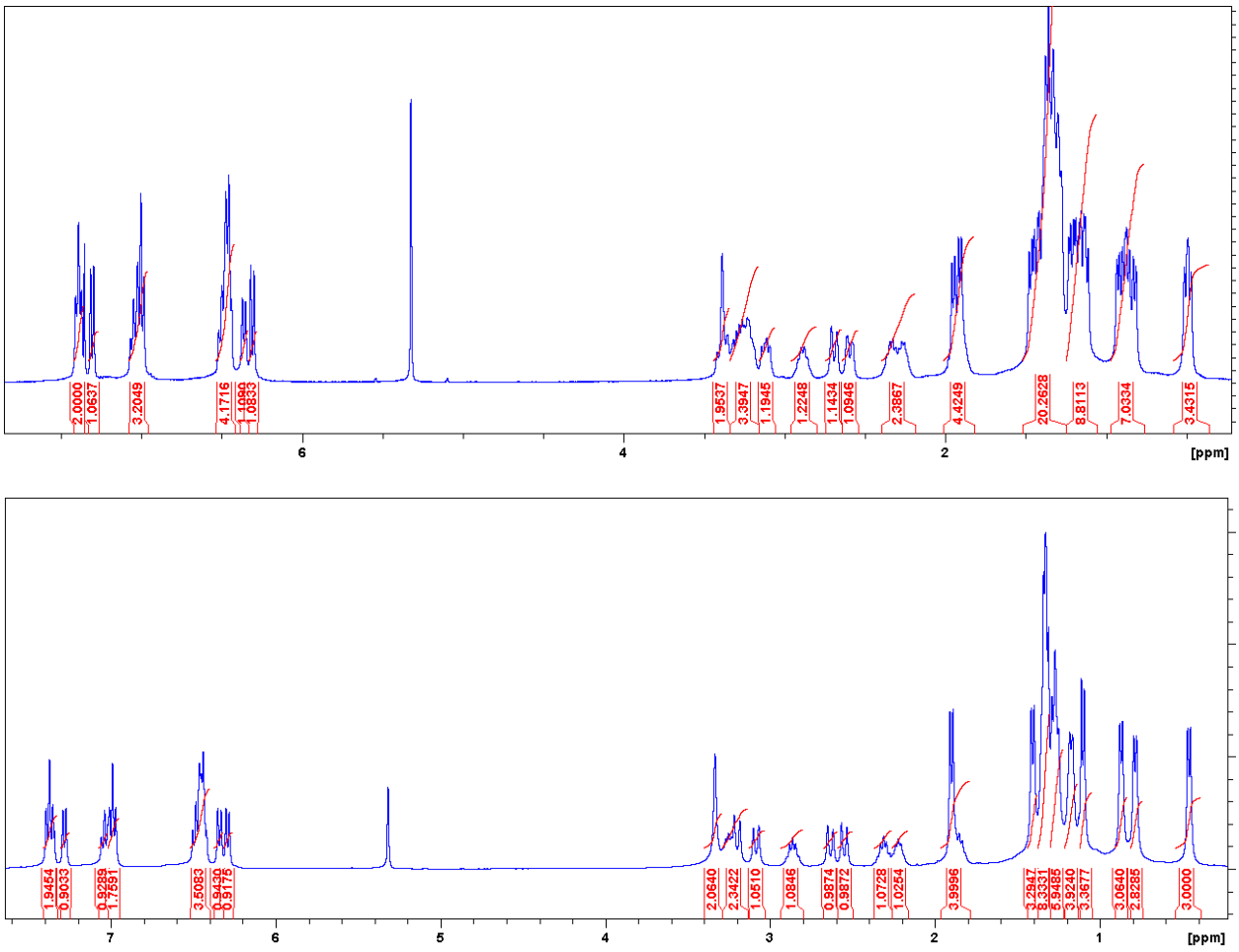

Figure S3. ^{1}H (top) and $^{1}H\{^{31}P\}$ (bottom) NMR spectra of **1-Cl** (400 MHz) in CD_2Cl_2 at -18°C.

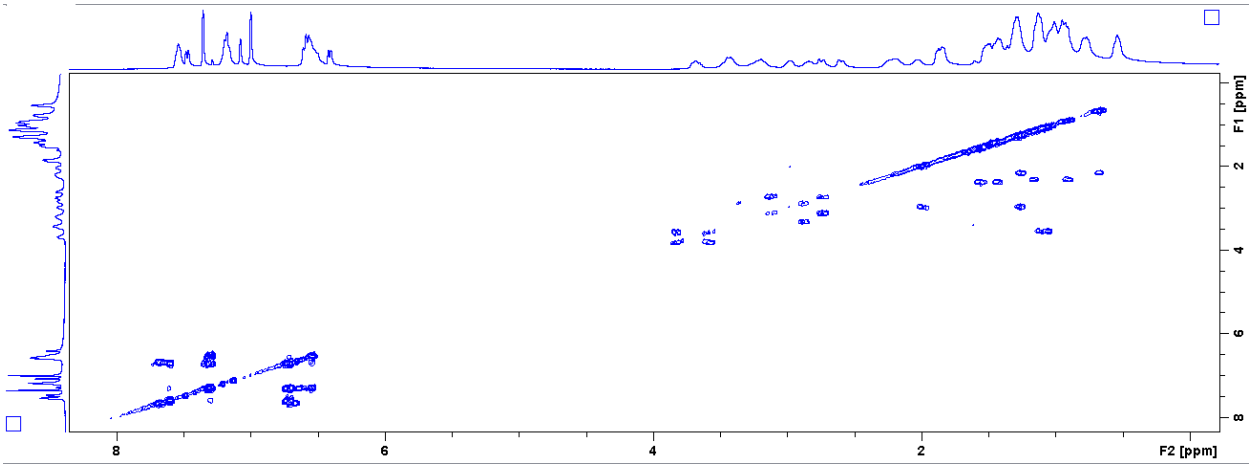

Figure S4. ^{1}H COSY NMR spectrum of **1-Cl** (400 MHz) in C_6D_5Br at 0°C.

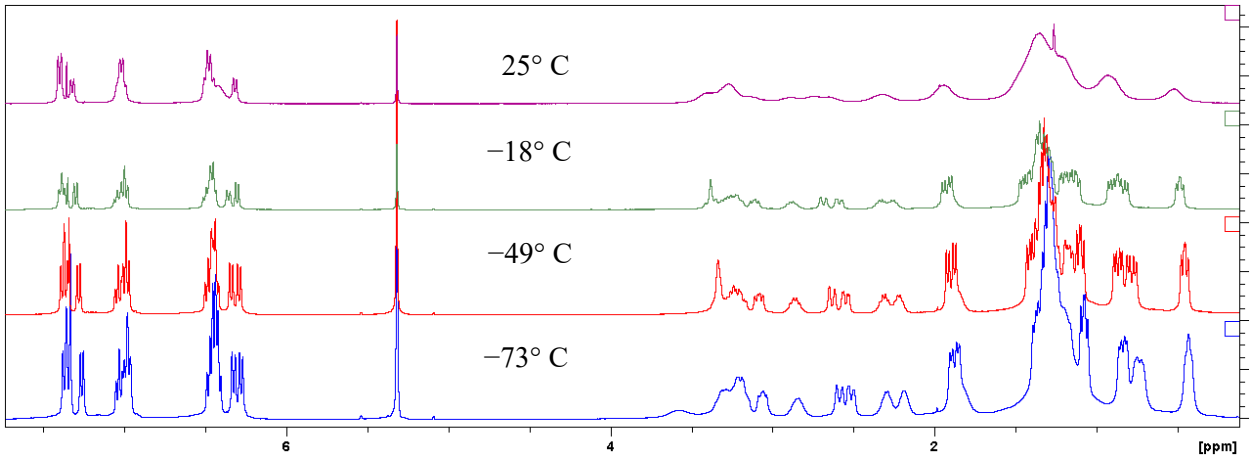

Figure S5. Low temperature VT ^{1}H NMR spectrum of **1-Cl** (400 MHz) in CD_2Cl_2. In order from bottom to top: −73°C, −49°C, −18°C, and 25°C.

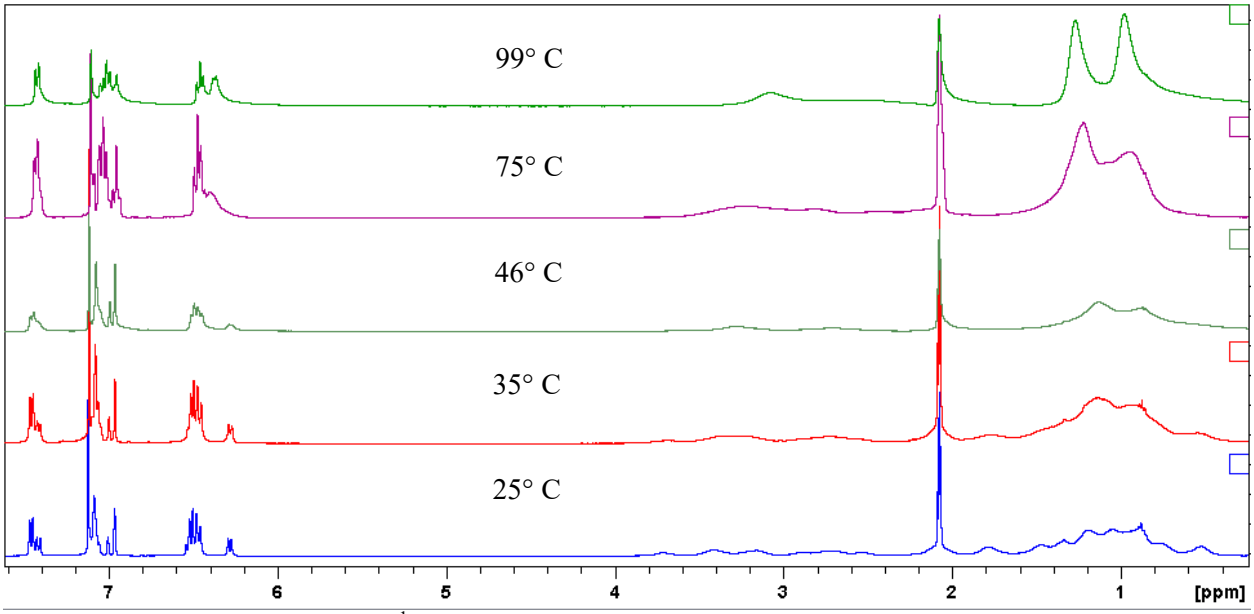

Figure S6. High temperature VT ^{1}H NMR spectrum of **1-Cl** (400 MHz) in toluene- d_8.

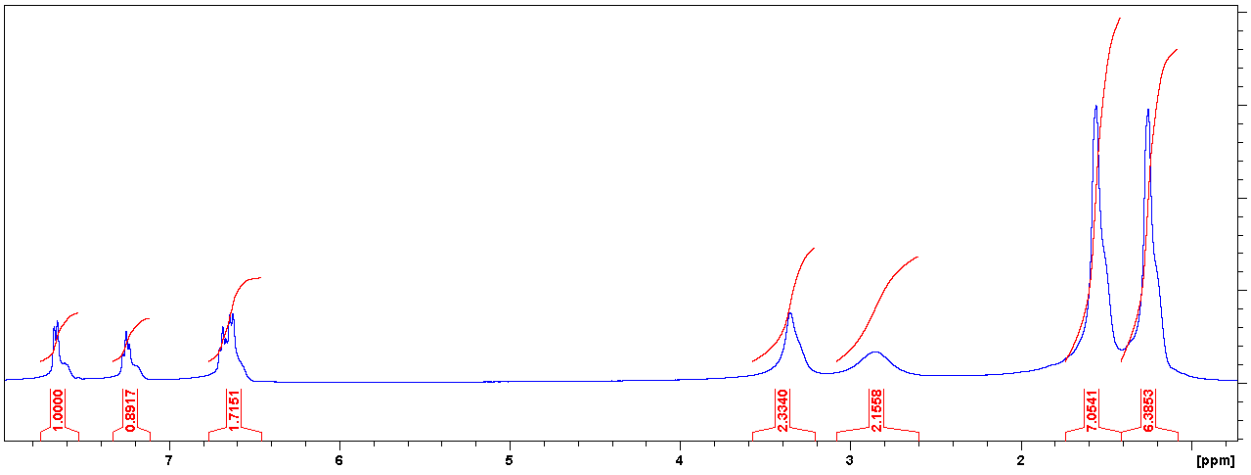

Figure S7. ^{1}H NMR spectrum of **1-Cl** (400 MHz) in C_6D_5Br at 115°C. The bad shims are an effect of the shimming coils being at an elevated temperature.

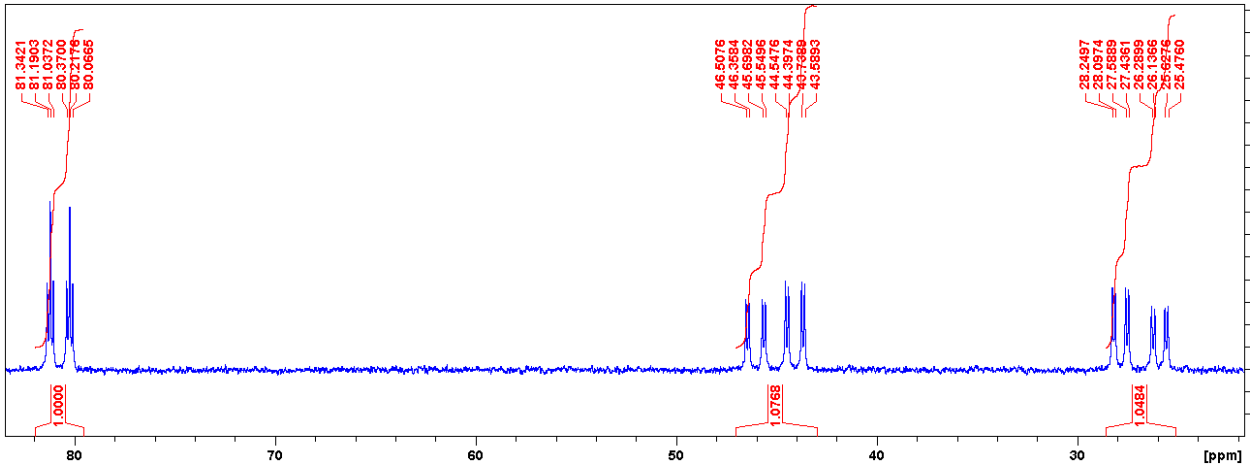

Figure S8. ^{31}P{^{1}H} NMR spectrum of **1-Cl** (162 MHz) in CD_2Cl_2 at −18°C.

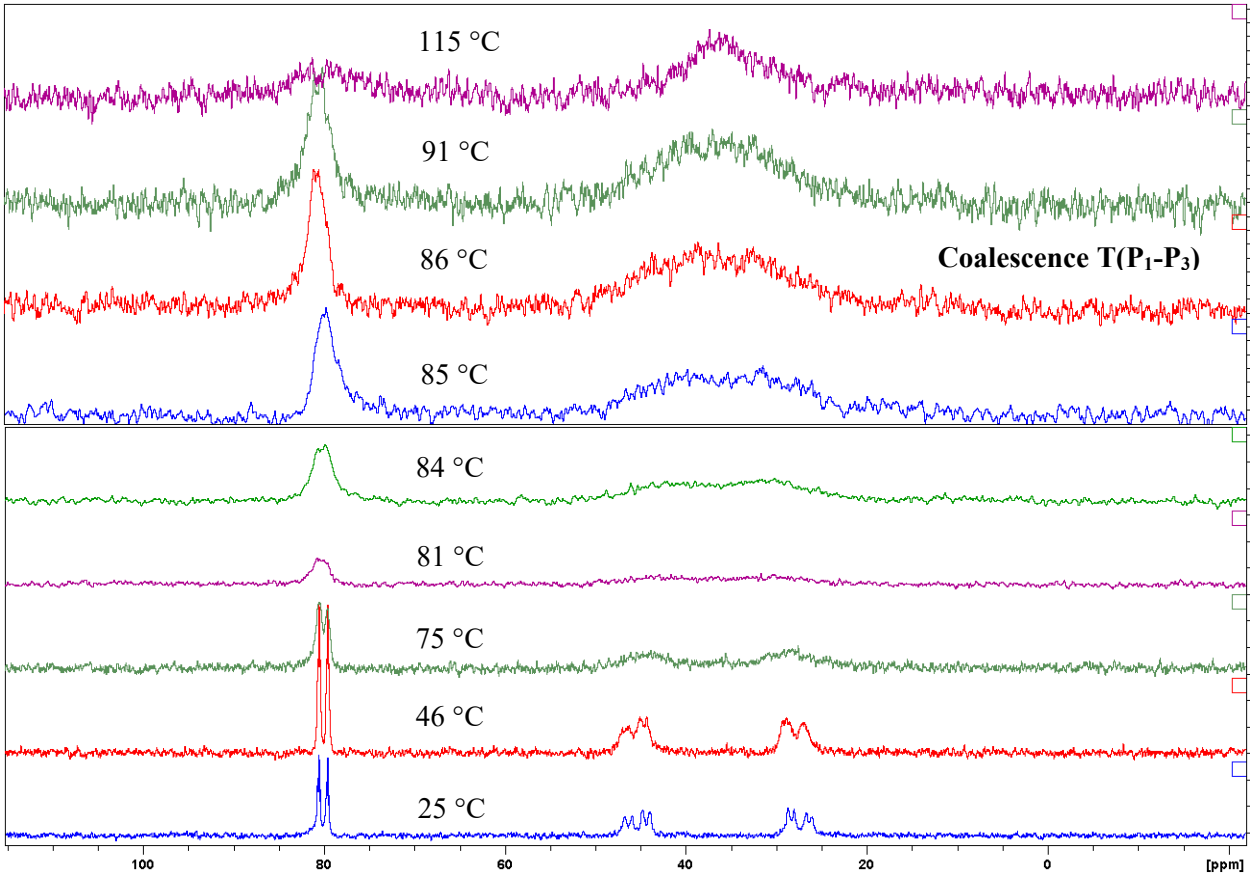

Figure S9. High temperature VT $^{31}P\{^{1}H\}$ NMR spectra of **1-Cl** (162 MHz) in C_6D_5Br.

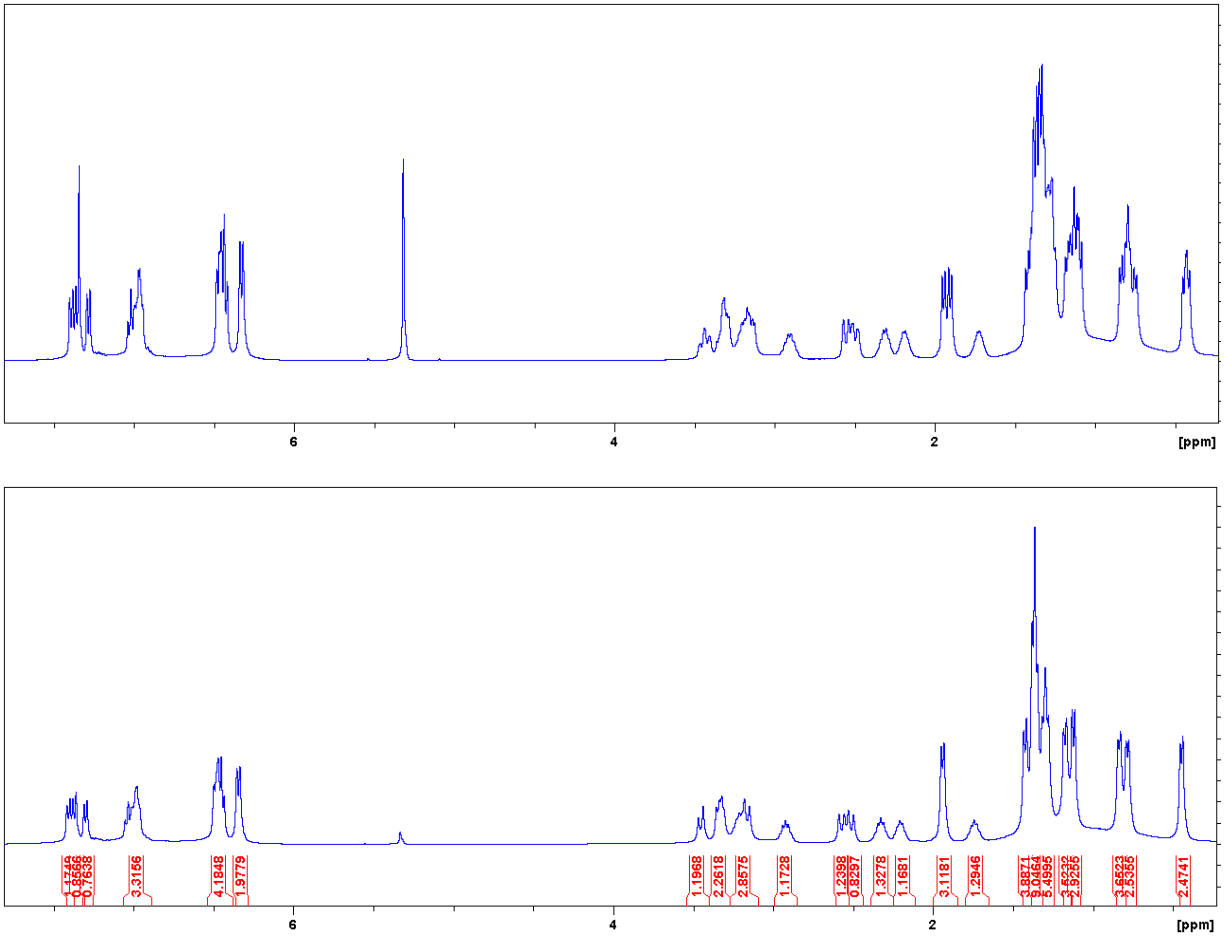

Figure S10. ^{1}H (top) and $^{1}H\{^{31}P\}$ (bottom) NMR spectra of **2-Cl** (400 MHz) in CD_2Cl_2 at −49°C.

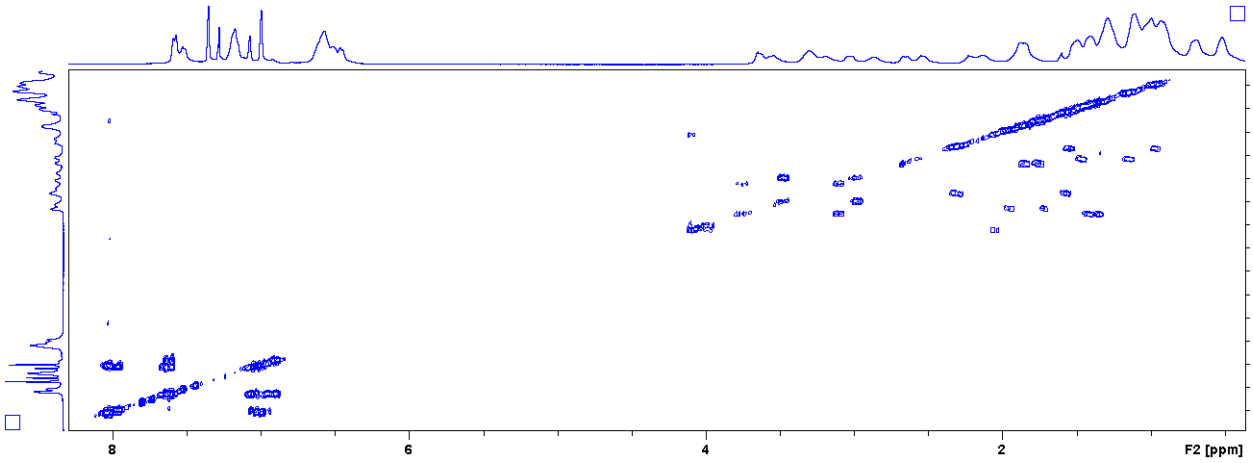

Figure S11. ^{1}H COSY NMR spectrum of **2-Cl** (400 MHz) in C_6D_5Br at 0°C.

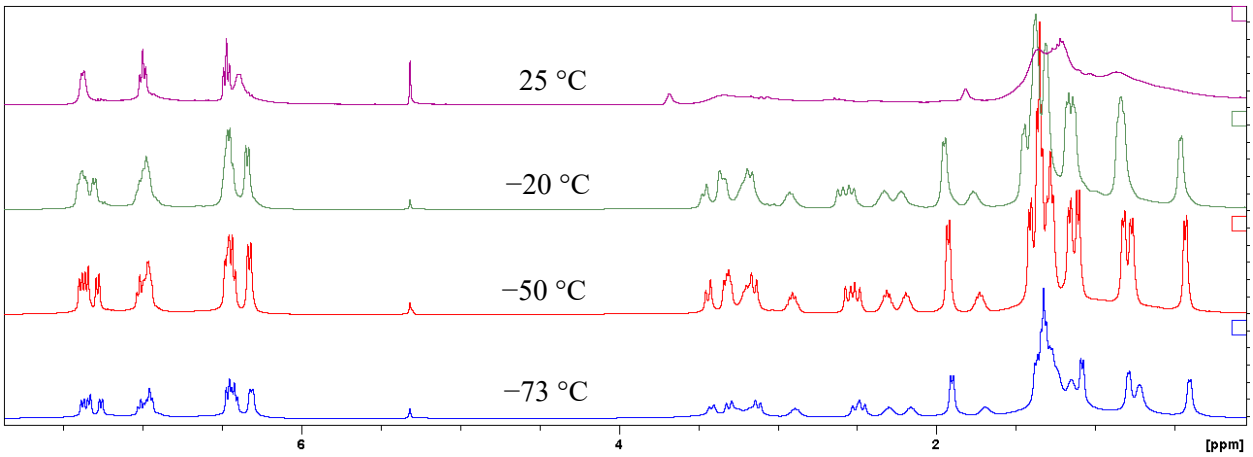

Figure S12. Low temperature VT ^{1}H NMR spectrum of **2-Cl** (400 MHz) in CD_2Cl_2.

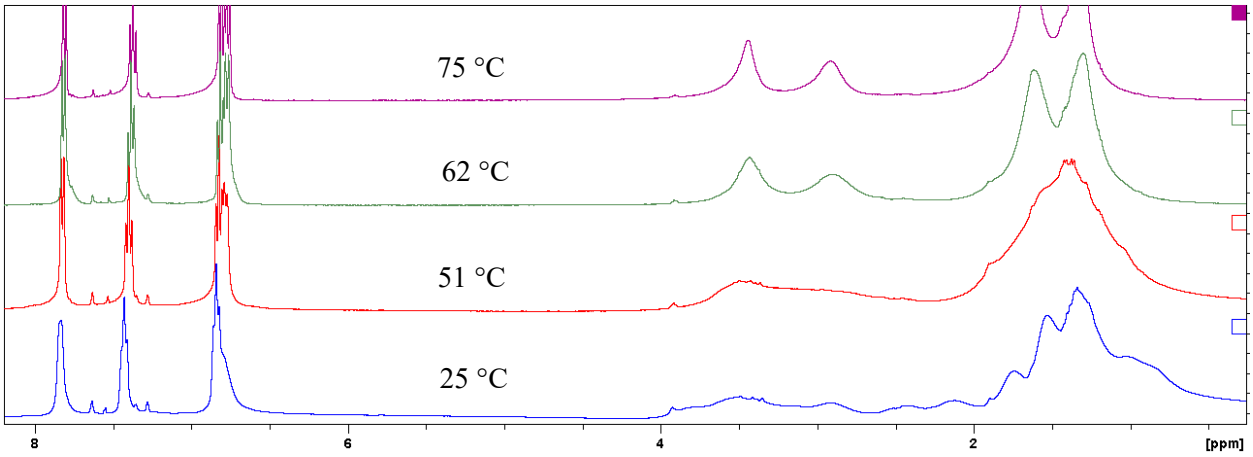

Figure S13. High temperature VT ^{1}H NMR spectrum of **2-Cl** (400 MHz) in C_6D_5Br.

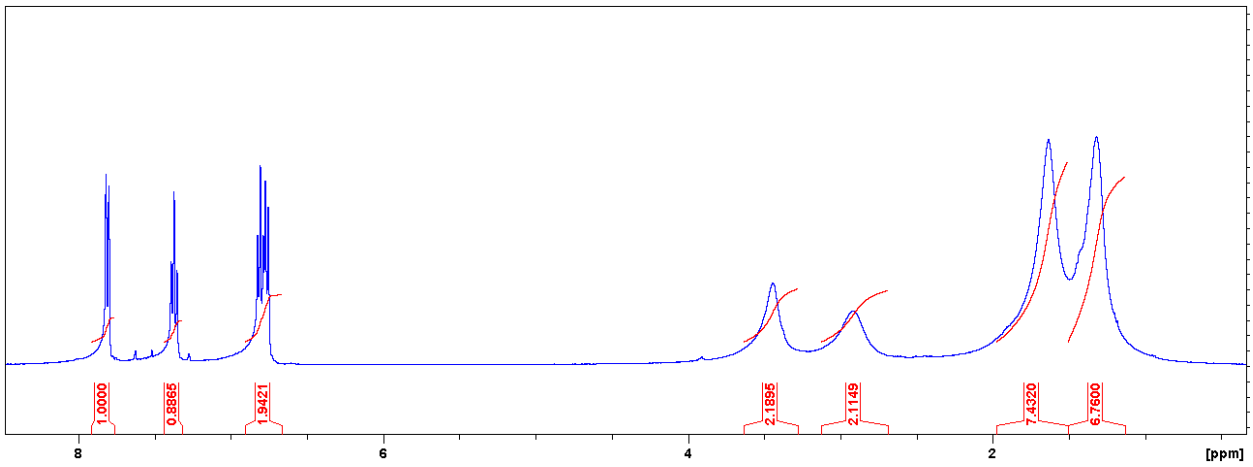

Figure S14. ^{1}H NMR spectrum of **2-Cl** (400 MHz) in C_6D_5Br at 75°C.

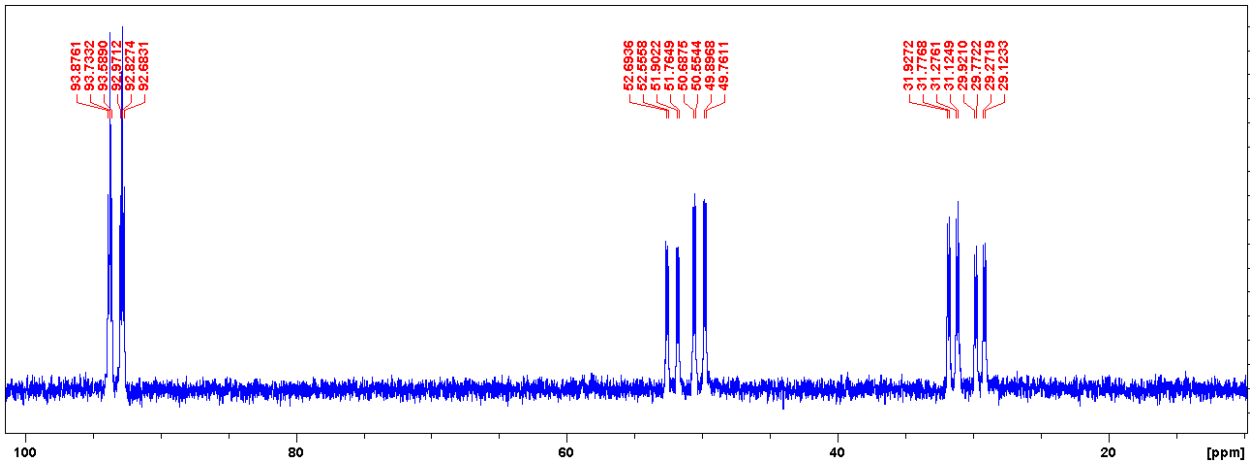

Figure S15. $^{31}P\{^{1}H\}$ NMR spectrum of **2-Cl** (162 MHz) in CD_2Cl_2 at −18°C.

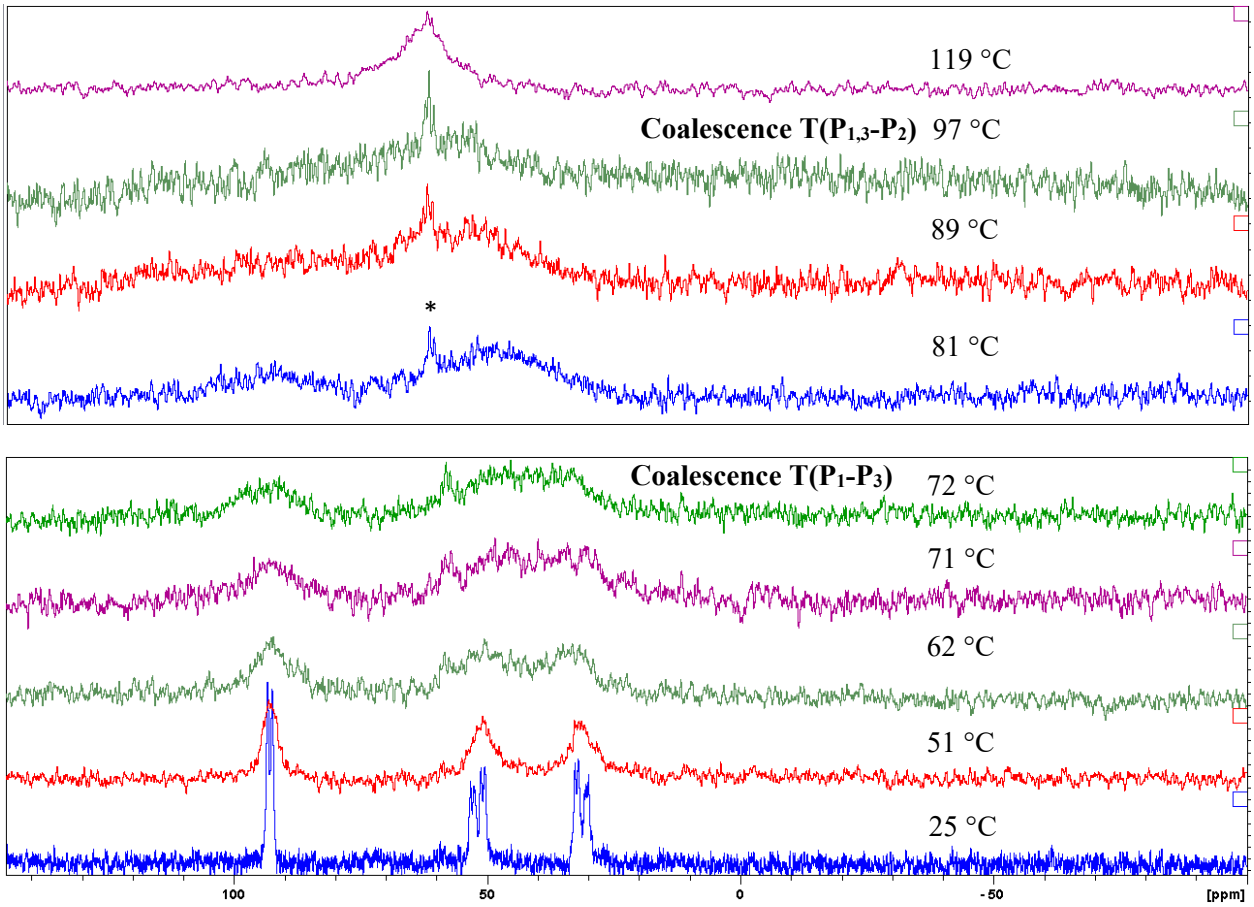

Figure S16. High temperature VT $^{31}P\{^{1}H\}$ NMR spectra of **2-Cl** (162 MHz) in C_6D_5Br. * denote a minor impurity. Note: The average of the three peaks at -18°C: (93.3 + 51.2 + 30.5)/3 = 58.3 ppm, which is close to the 58.6 ppm shift observed at high temperatures.

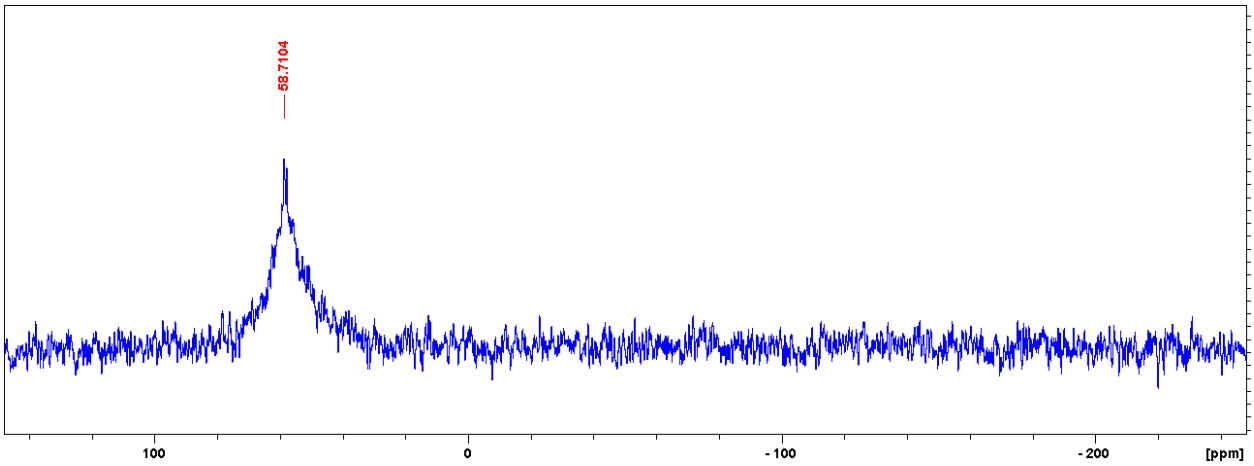

Figure S17. $^{31}P\{^{1}H\}$ NMR spectrum of **2-Cl** (162 MHz) in C_6D_5Br at 107°C.

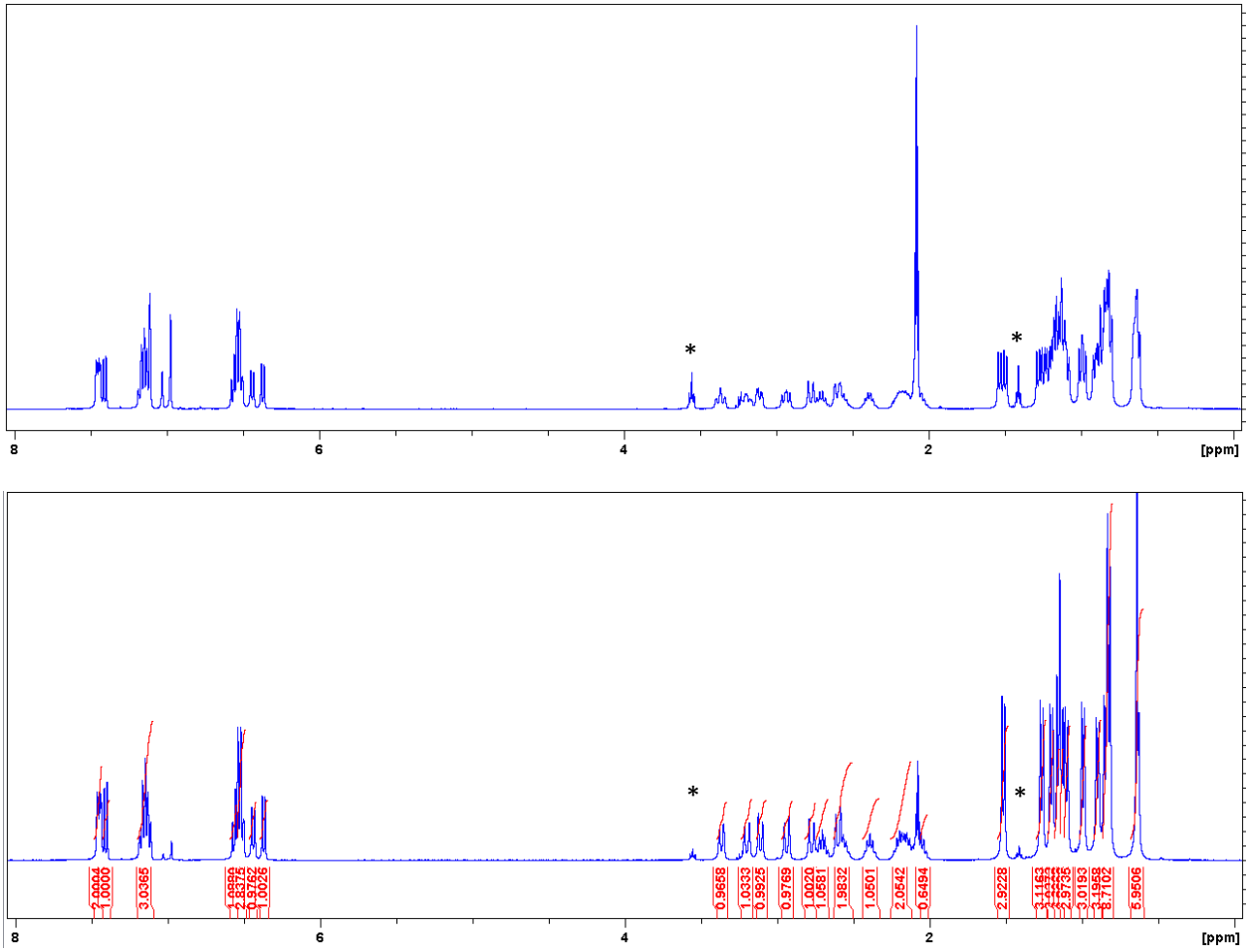

Figure S18. ^{1}H (top) and $^{1}H\{^{31}P\}$ (bottom) NMR spectra of **1-CH$_3$** (400 MHz) in toluene-d_8 at −18°C. * denotes residual THF.

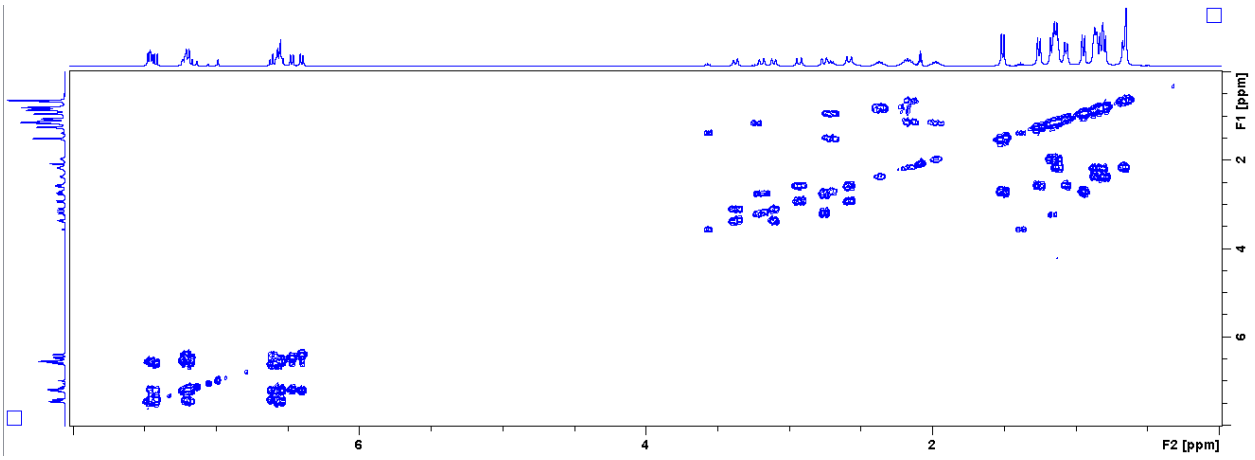

Figure S19. ^{1}H COSY NMR spectrum of **1-CH$_3$** (400 MHz) in toluene- d_8 at −18°C.

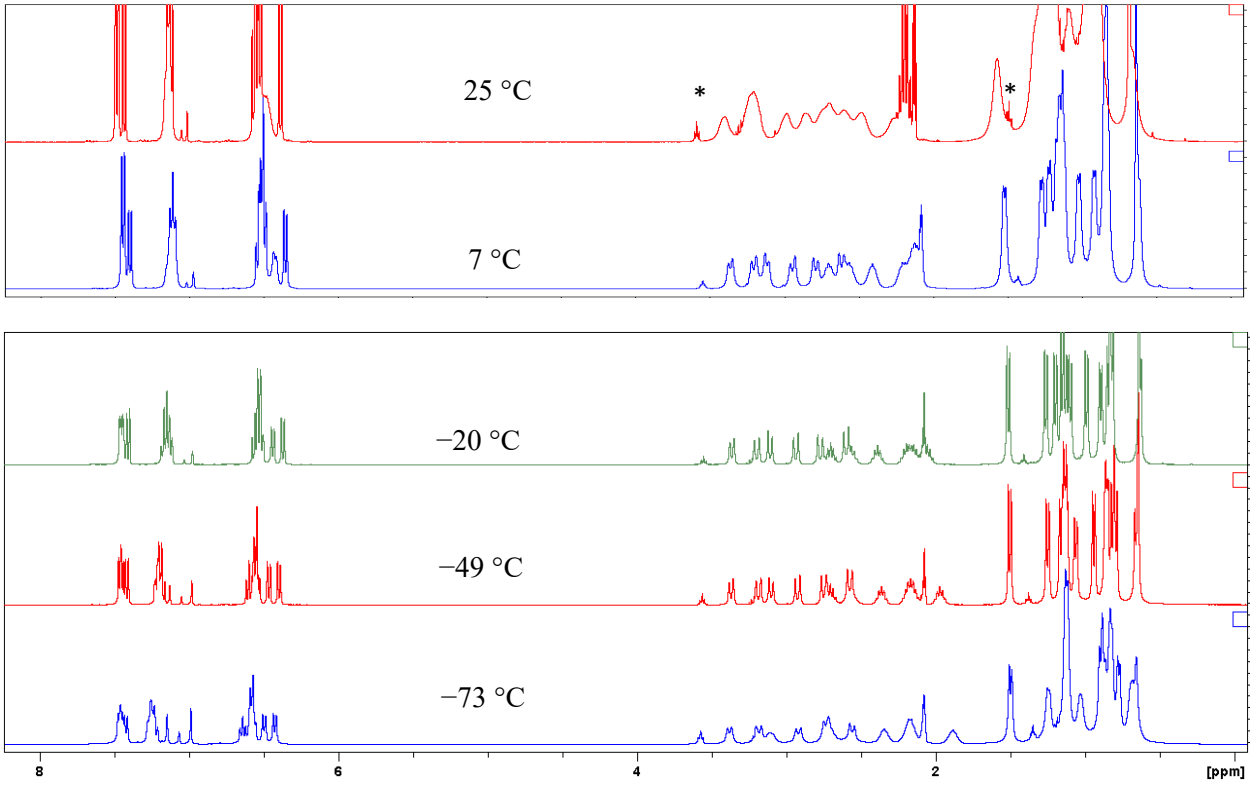

Figure S20. Low temperature VT ^{1}H{^{31}P} NMR spectrum of **1-CH$_3$** (400 MHz) in toluene-d_8. * denotes residual THF.

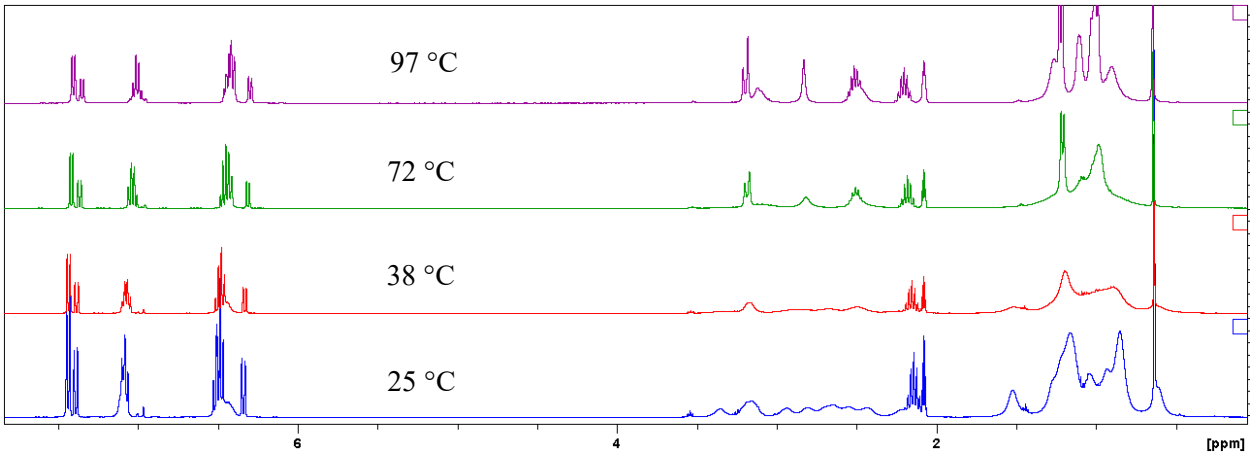

Figure S21. High temperature VT ^{1}H NMR spectrum of **1-CH$_3$** (400 MHz) in toluene- d_8.

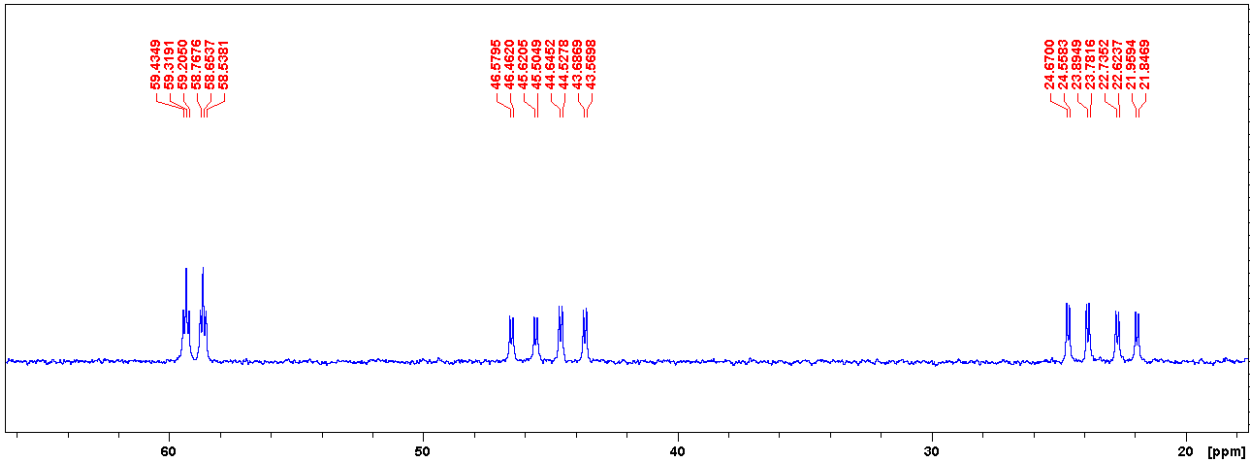

Figure S22. ^{31}P{^{1}H} NMR spectrum of **1-CH$_3$** (162 MHz) in toluene-d_8 at −18°C.

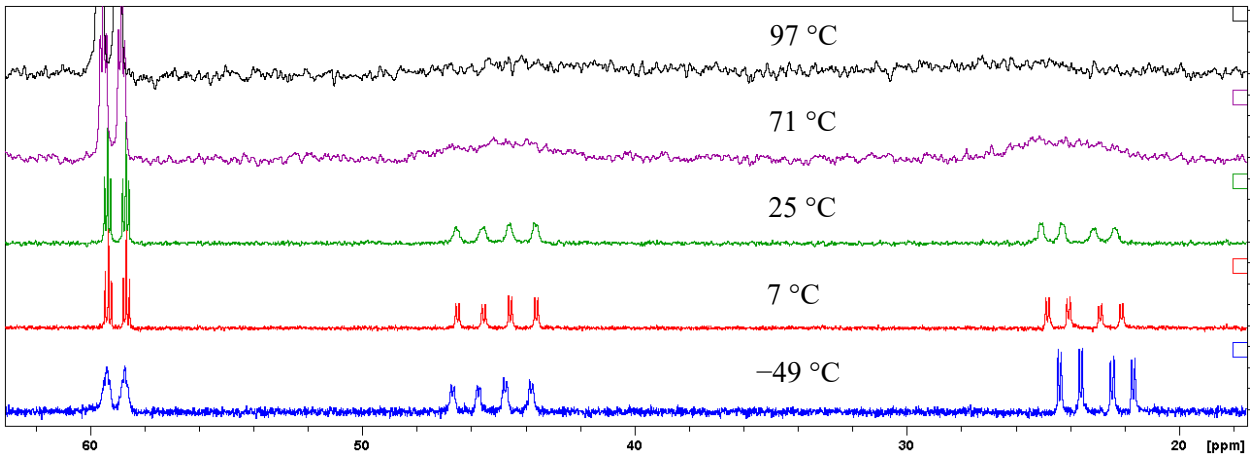

Figure S23. VT $^{31}P\{^{1}H\}$ NMR spectra of **1-CH$_3$** (162 MHz) in toluene-d_8.

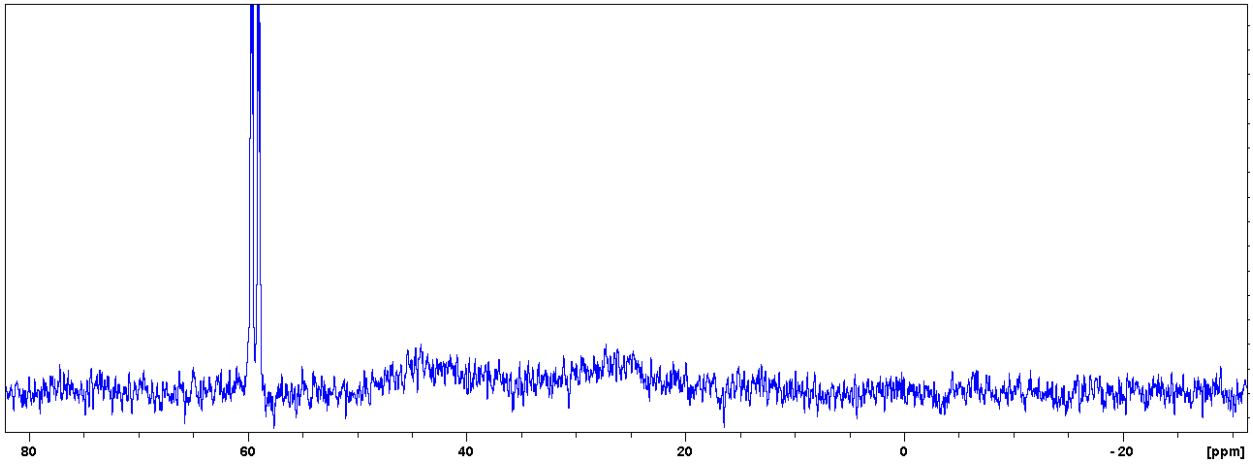

Figure S24. $^{31}P\{^{1}H\}$ NMR spectrum of **1-CH$_3$** (162 MHz) in toluene-d_8 at 97°C. The peaks for P_1 and P_3 have not yet coalesced at this temperature.

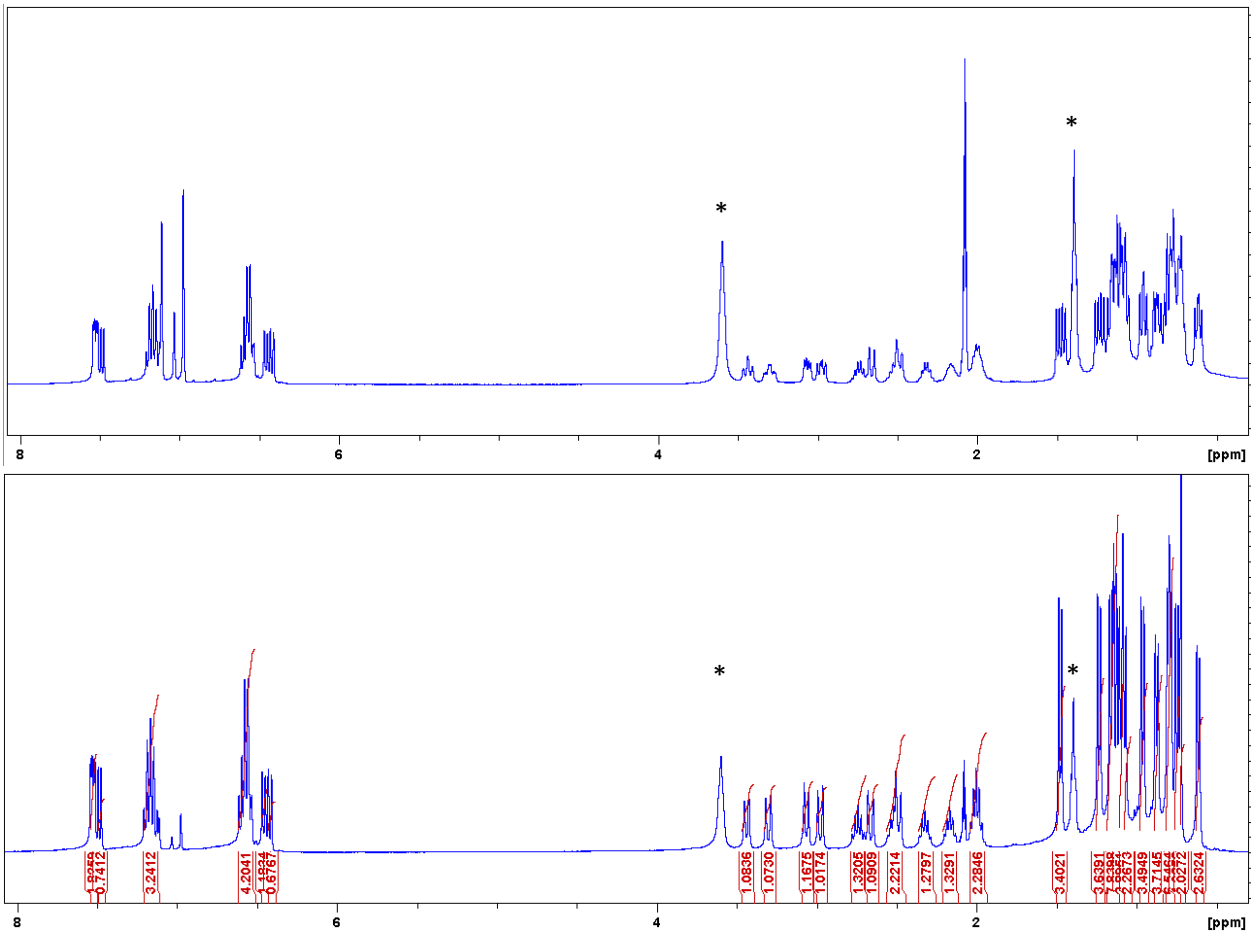

Figure S25. ^{1}H (top) and $^{1}H\{^{31}P\}$ (bottom) NMR spectra of **2-CH$_3$** (400 MHz) in toluene-d_8 at −13°C. * denotes residual THF.

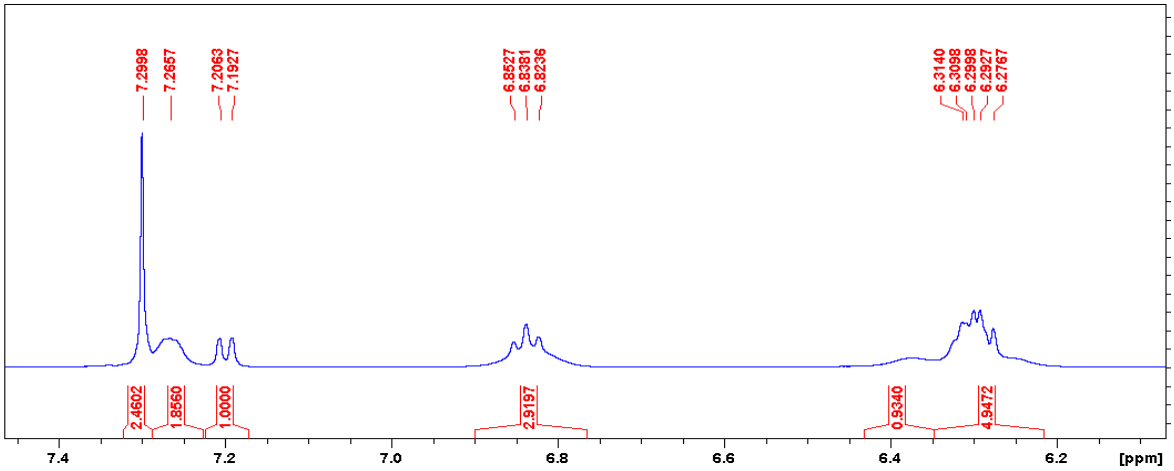

Figure S26. ^{1}H NMR spectrum of **2-CH$_3$** sample sent for elemental analysis in THF-d_8. Crystals of **2-CH$_3$**·(C_6H_6) was subjected to vacuum prior to elemental analysis (EA). The NMR of the aryl region for the EA sample shows that the relative integration of C_6H_6 to **2-CH$_3$** is 0.5 to 1.

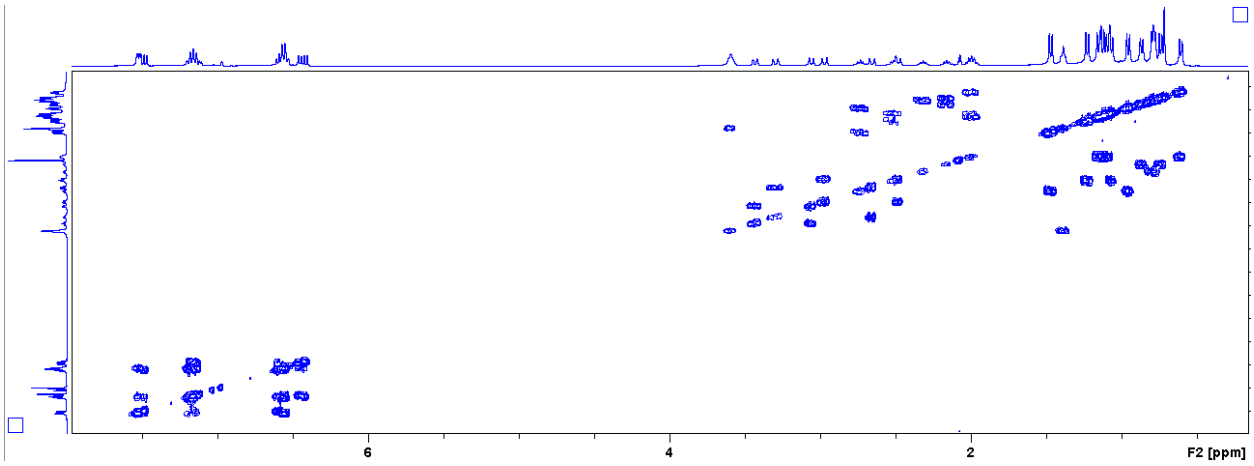

Figure S27. ^{1}H COSY NMR spectrum of **2-CH$_3$** (400 MHz) in toluene-d_8 at −13°C.

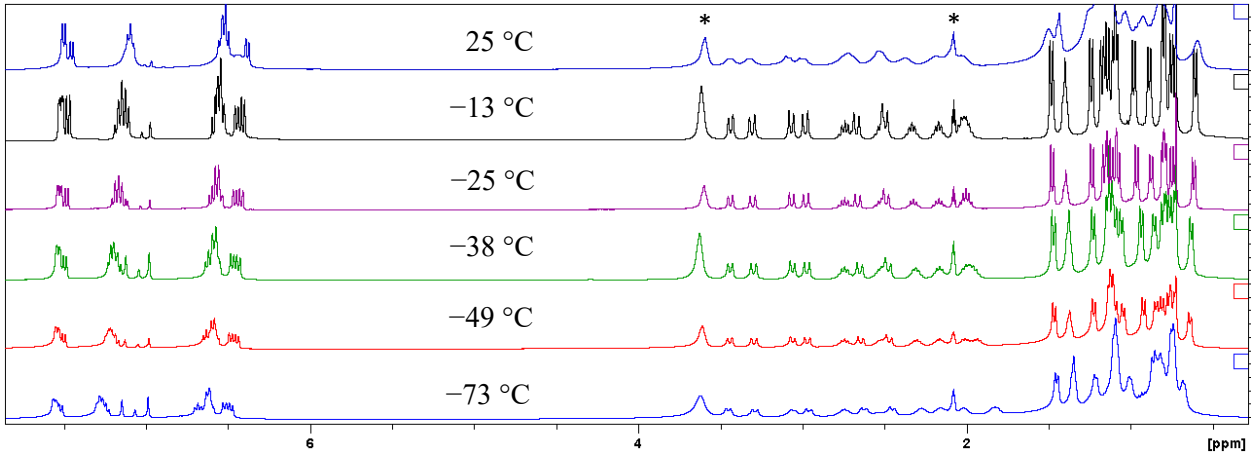

Figure S28. Low temperature VT ^{1}H{^{31}P} NMR spectrum of **2-CH$_3$** (400 MHz) in toluene- d_8. * denotes residual THF.

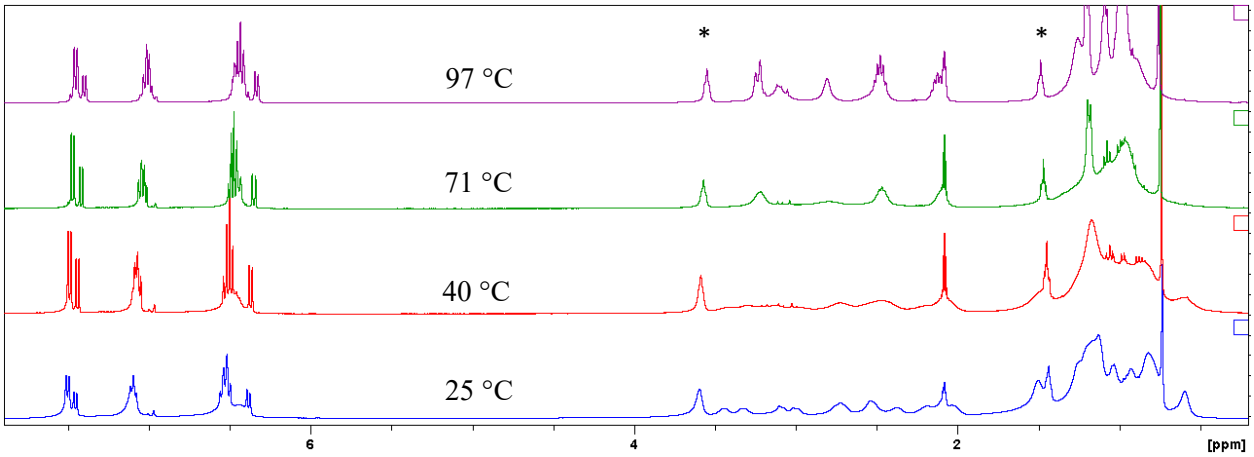

Figure S29. High temperature VT ^{1}H{^{31}P} NMR spectrum of **2-CH$_3$** (400 MHz) in toluene- d_8. * denotes residual THF.

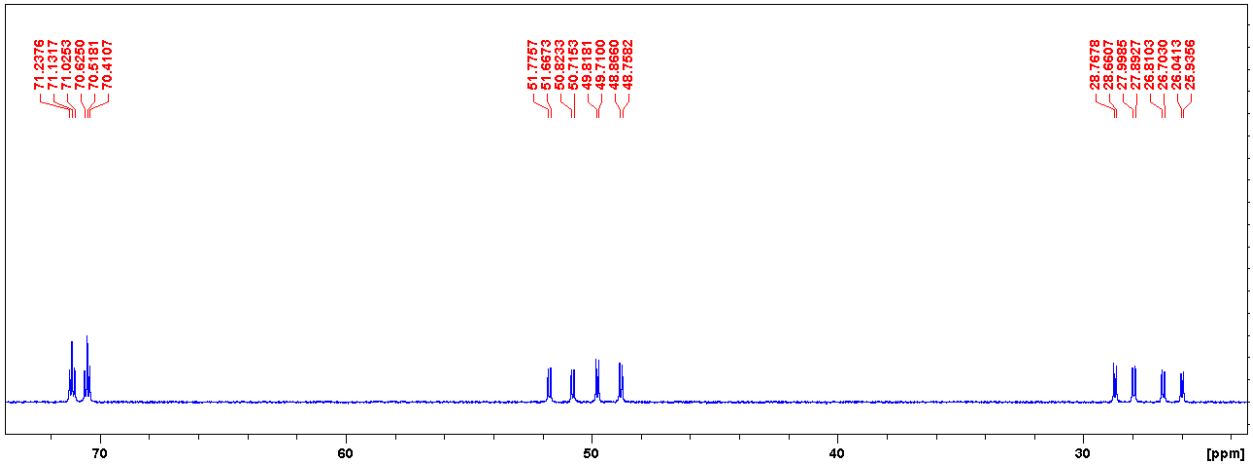

Figure S30. $^{31}P\{^{1}H\}$ NMR spectrum of **2-CH$_3$** (162 MHz) in toluene- d_8 at 3°C.

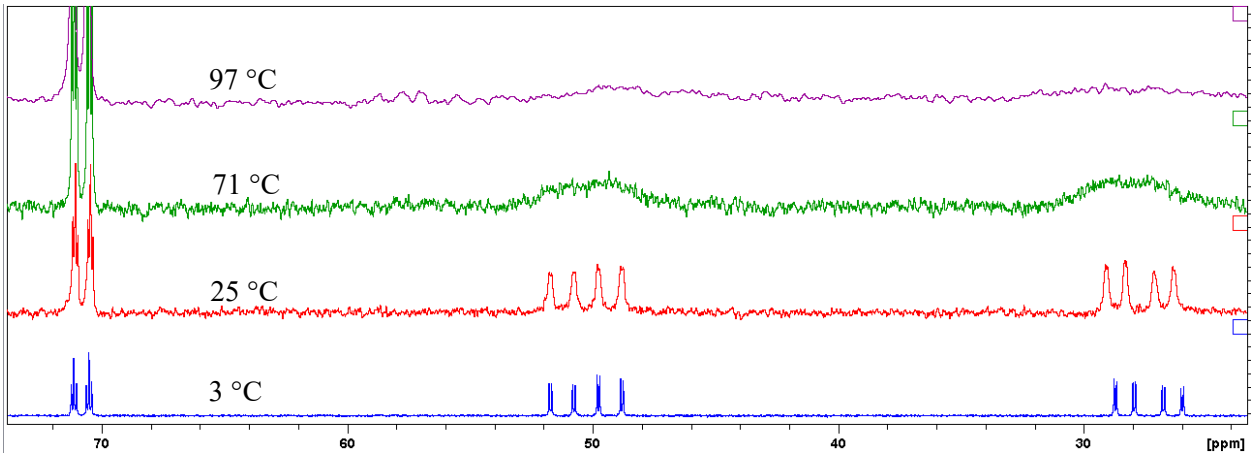

Figure S31. VT $^{31}P\{^{1}H\}$ NMR spectra of **2-CH$_3$** (162 MHz) in toluene- d_8.

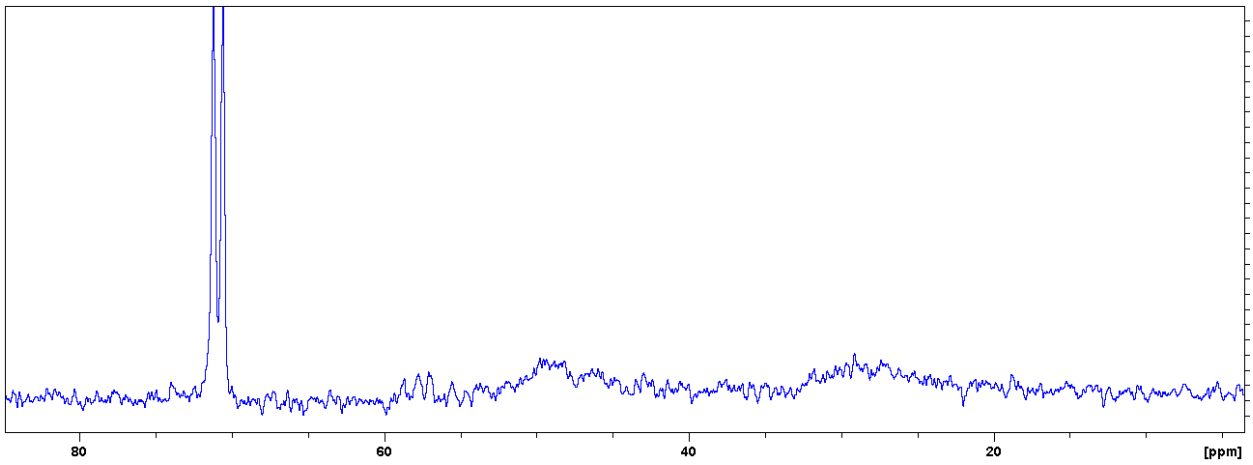

Figure S32. $^{31}P\{^{1}H\}$ NMR spectrum of **2-CH$_3$** (162 MHz) in toluene-d_8 at 97°C. The peaks for P_1 and P_3 have not yet coalesced at this temperature.

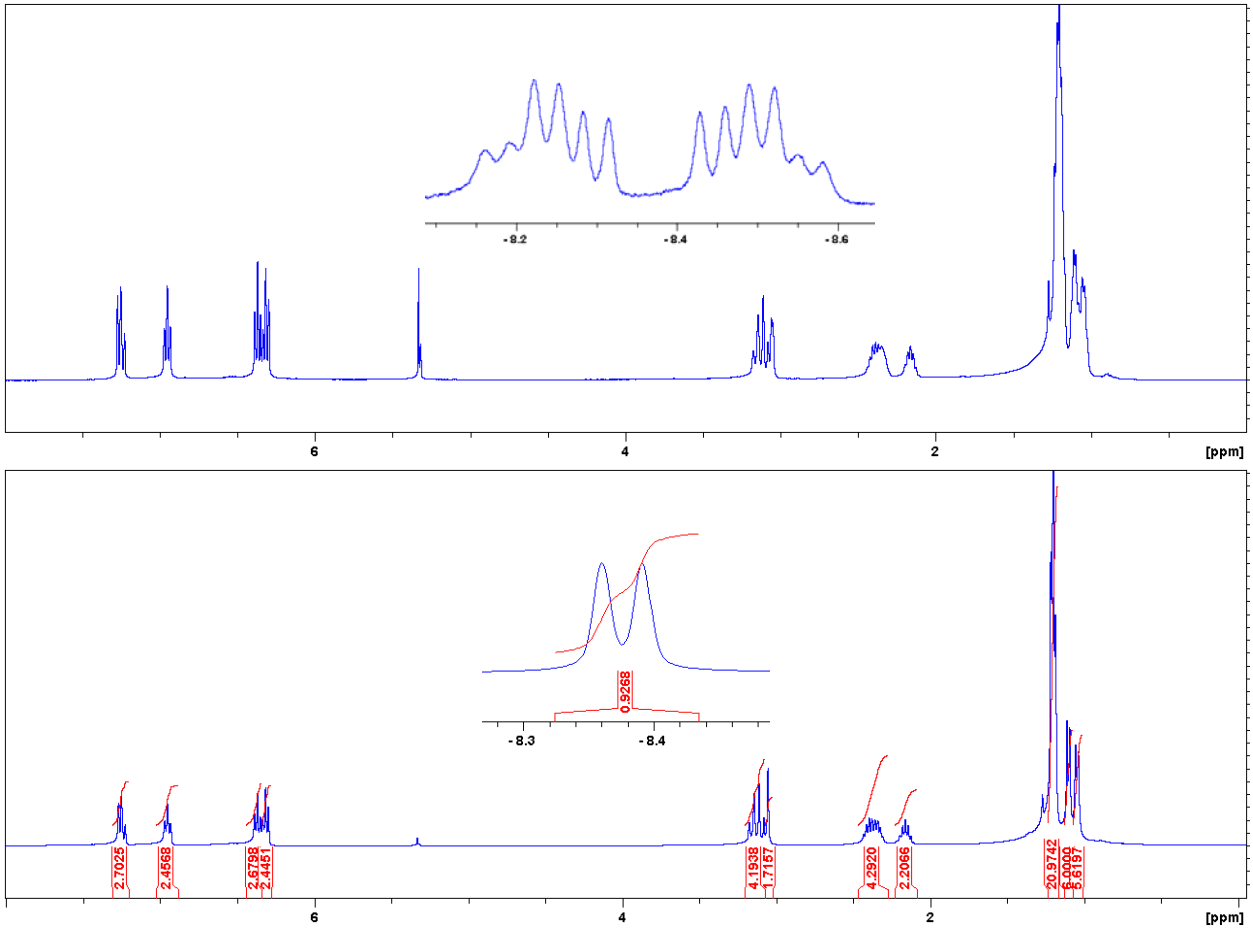

Figure S33. ^{1}H (top) and $^{1}H\{^{31}P\}$ (bottom) NMR spectra of **1-H** (400 MHz) in CD_2Cl_2 at 25°C.

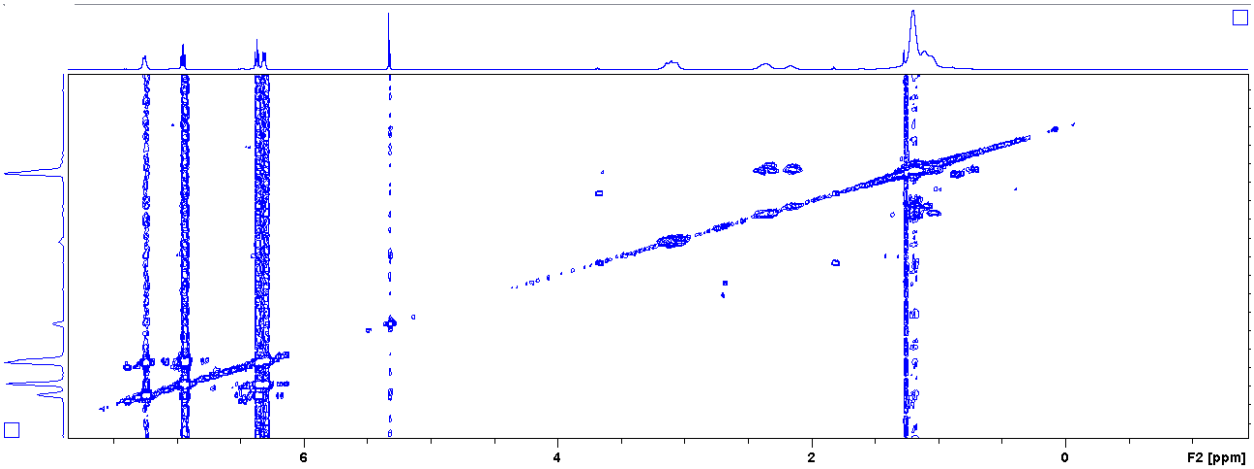

Figure S34. ^{1}H COSY NMR spectrum of **1-H** (500 MHz) in CD_2Cl_2 at 25°C.

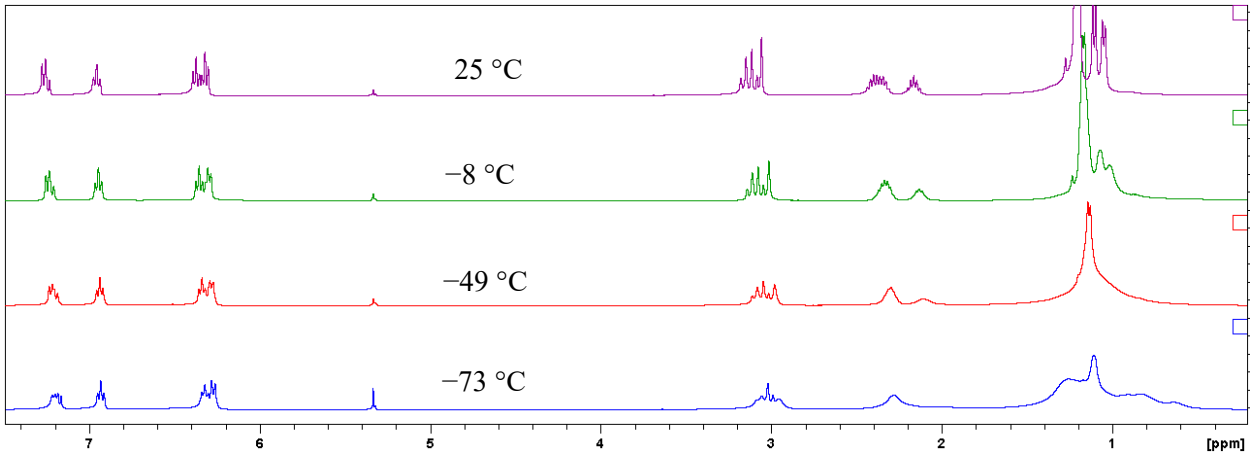

Figure S35. Low temperature VT $^{1}H\{^{31}P\}$ NMR spectrum of **1-H** (400 MHz) in CD_2Cl_2.

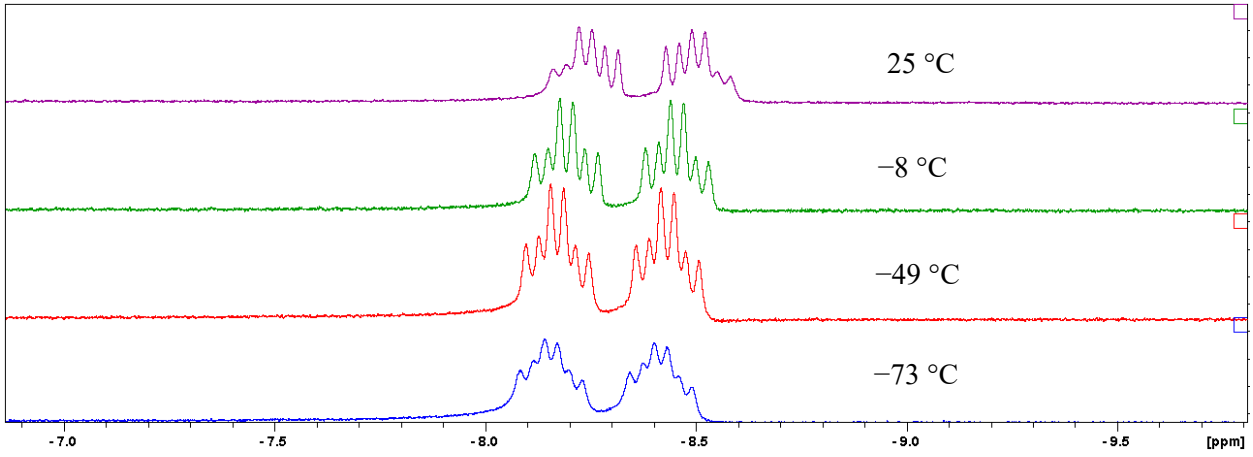

Figure S36. Low temperature VT $^{1}H\{^{31}P\}$ NMR spectrum of **1-H** (400 MHz) in CD_2Cl_2 in hydride region. In order from bottom to top: −73°C, −49°C, −8°C and 25°C.

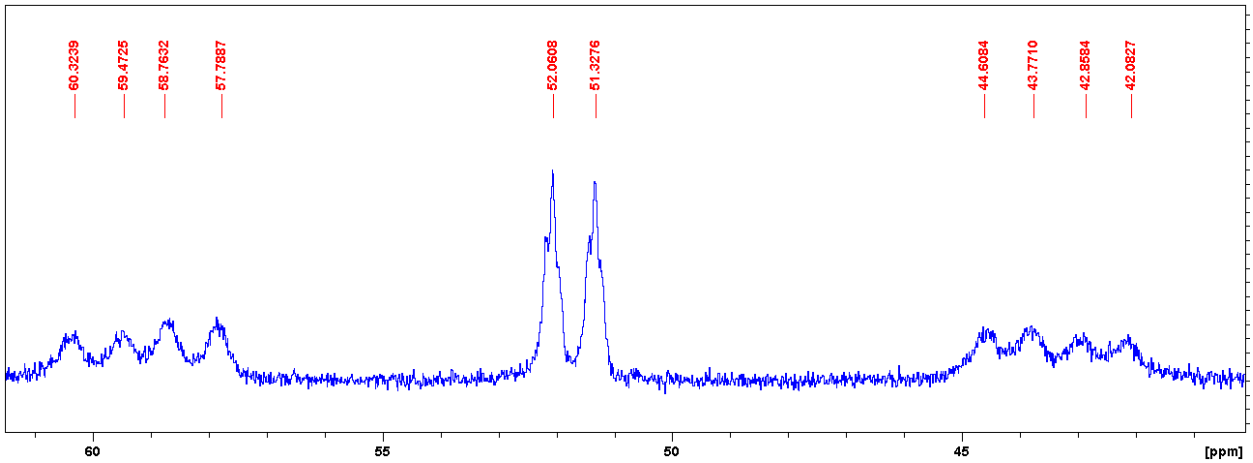

Figure S37. $^{31}P\{^{1}H\}$ NMR spectrum of **1-H** (162 MHz) in CD_2Cl_2 at −73°C.

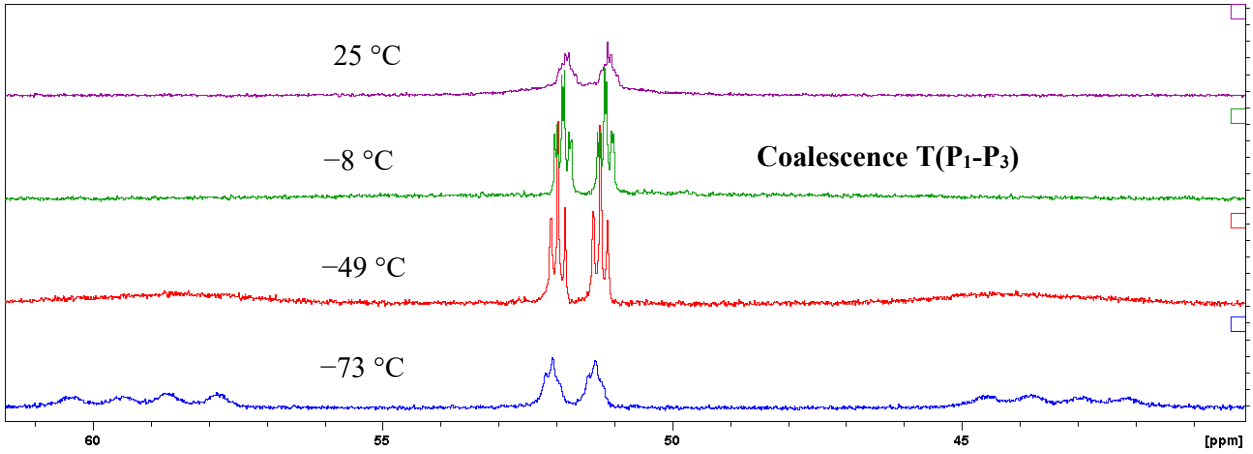

Figure S38. VT $^{31}P\{^{1}H\}$ NMR spectra of **1-H** (162 MHz) in CD_2Cl_2.

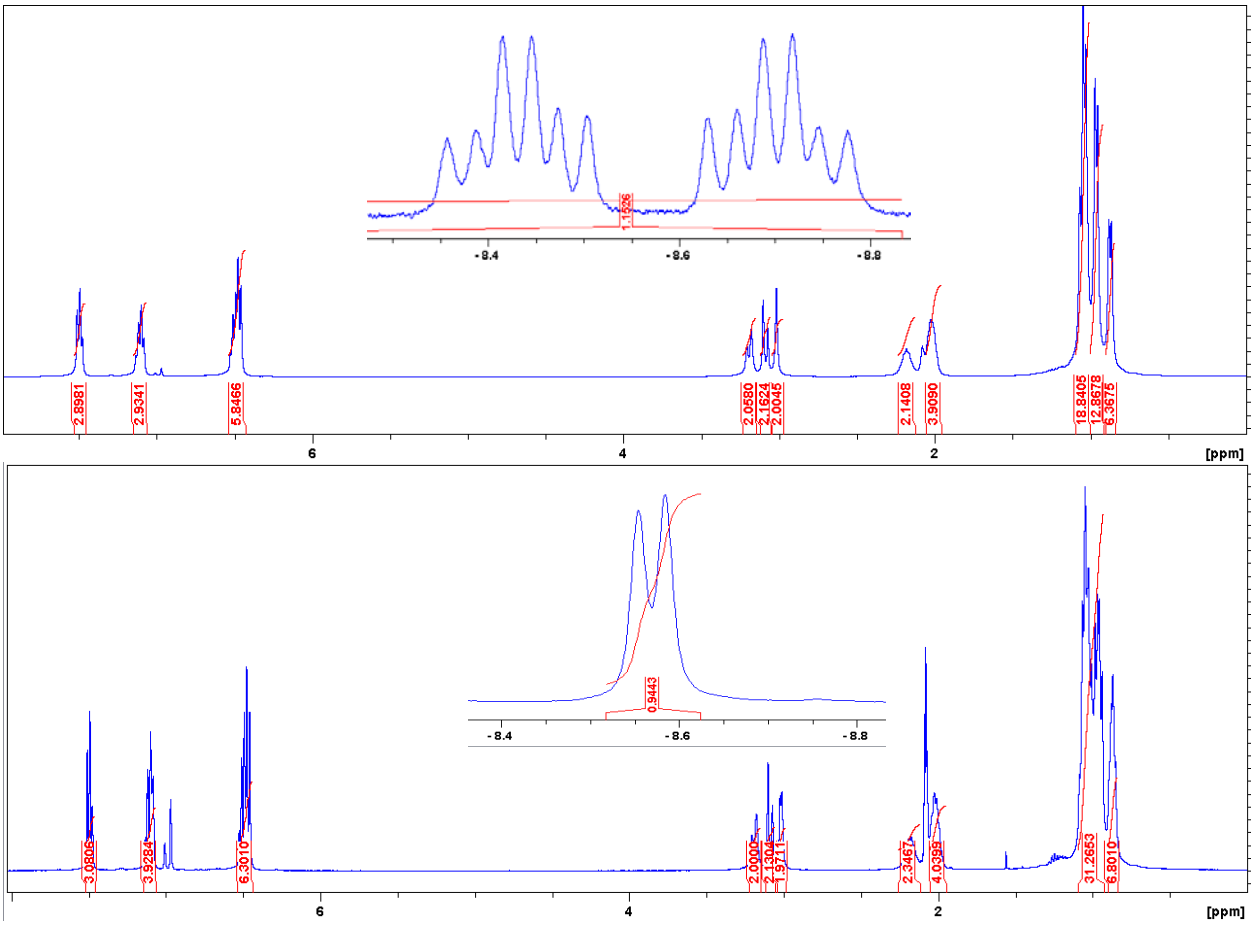

Figure S39. ^{1}H (top) and $^{1}H\{^{31}P\}$ (bottom) NMR spectra of **2-H** (400 MHz) in toluene-d_8 at 25°C.

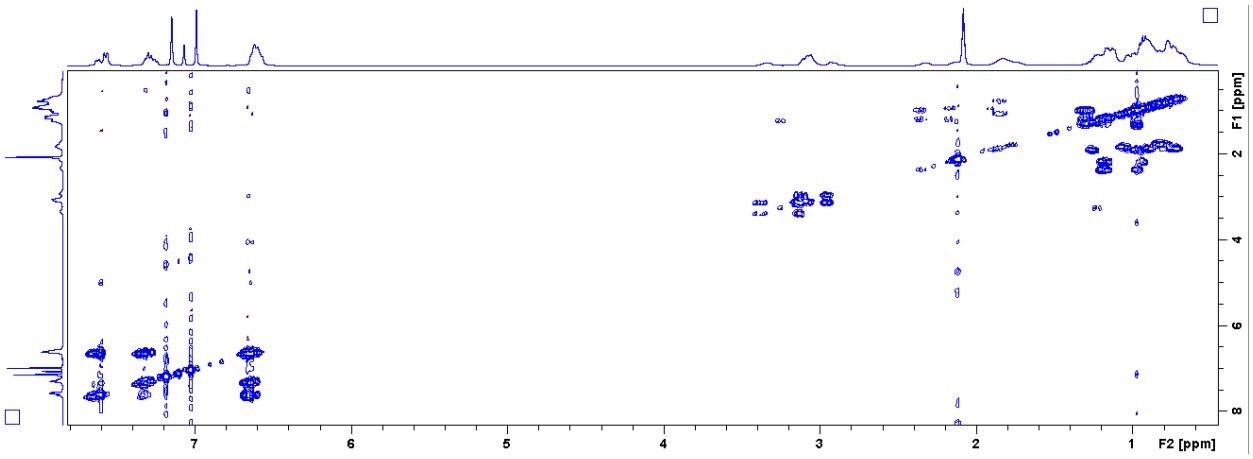

Figure S40. ^{1}H COSY NMR spectrum of **2-H** (400 MHz) in toluene- d_8 at −73°C.

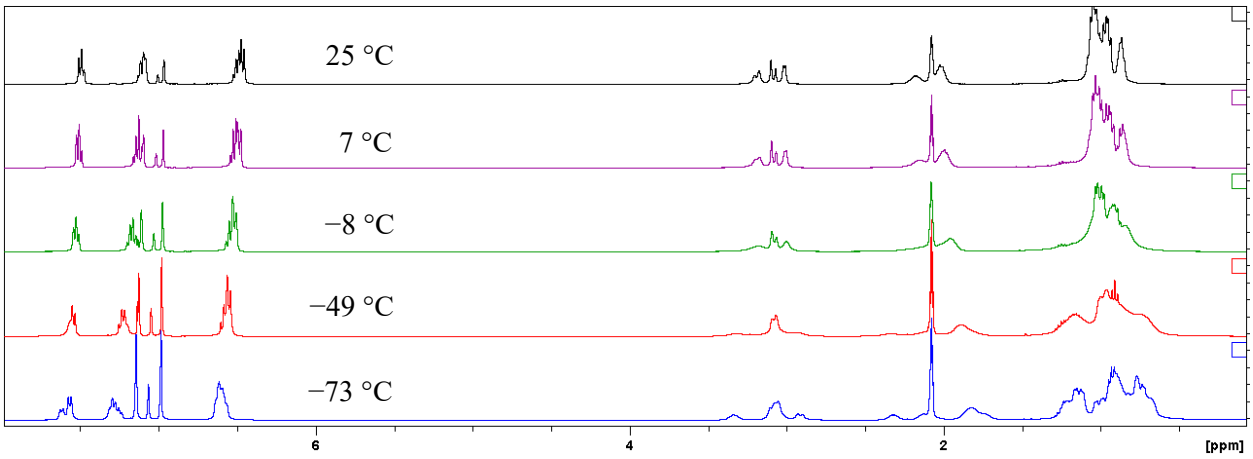

Figure S41. Low temperature VT ^{1}H{^{31}P} NMR spectrum of **2-H** (400 MHz) in toluene- d_8.

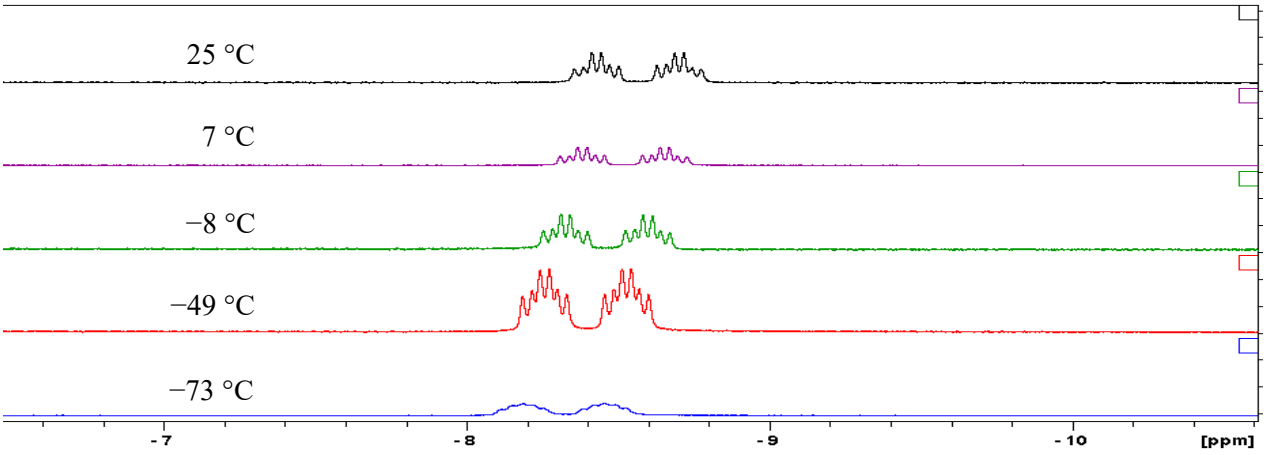

Figure S42. Low temperature VT ^{1}H{^{31}P} NMR spectrum of **2-H** (400 MHz) in toluene- d_8 in hydride region.

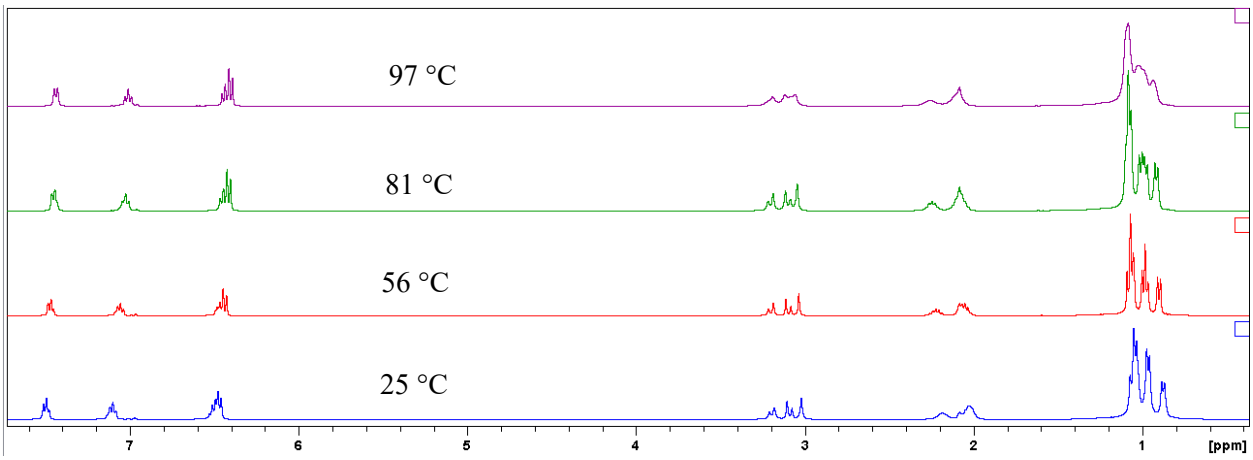

Figure S43. High temperature VT $^{1}H\{^{31}P\}$ NMR spectrum of **2-H** (400 MHz) in toluene- d_8.

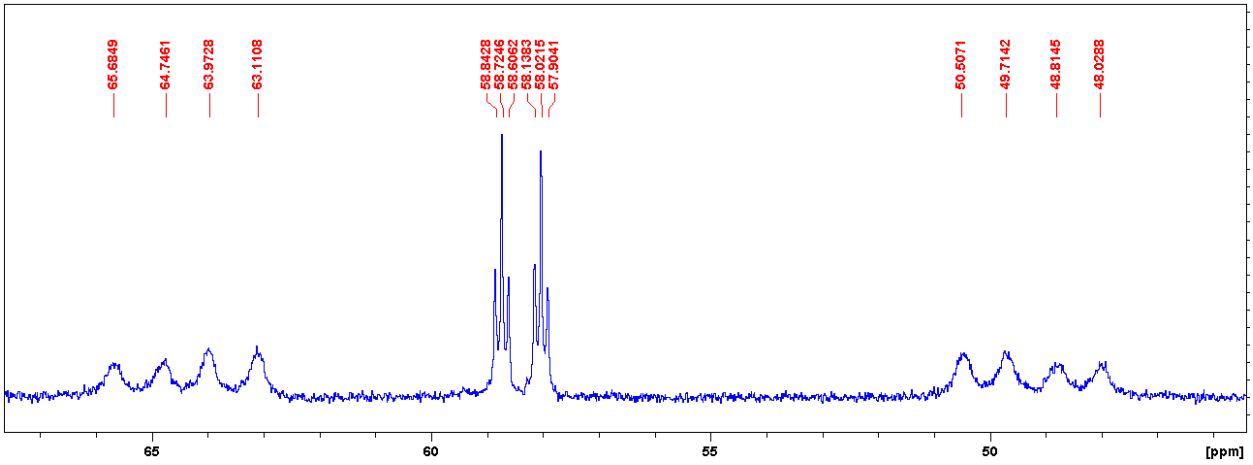

Figure S44. $^{31}P\{^{1}H\}$ NMR spectrum of **2-H** (162 MHz) in toluene- d_8 at −49°C.

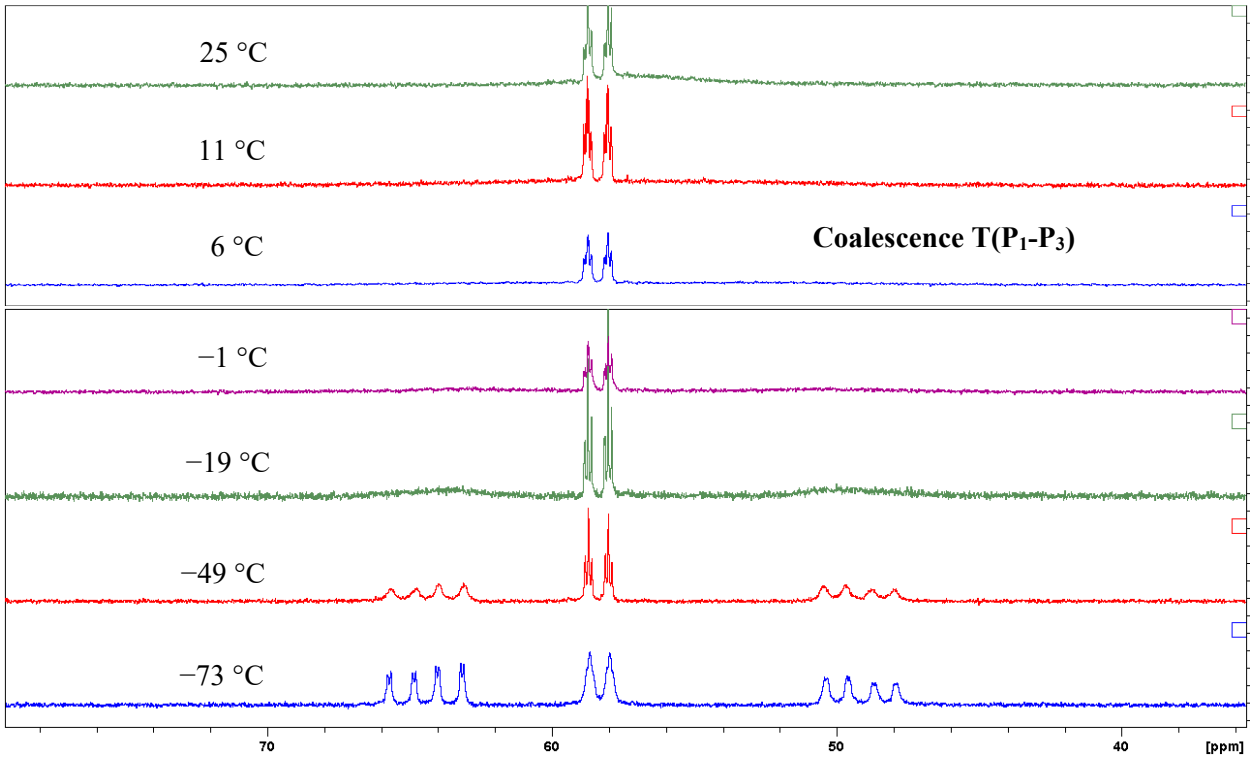

Figure S45. Low temperature VT $^{31}P\{^{1}H\}$ NMR spectra of **2-H** (162 MHz) in toluene- d_8.

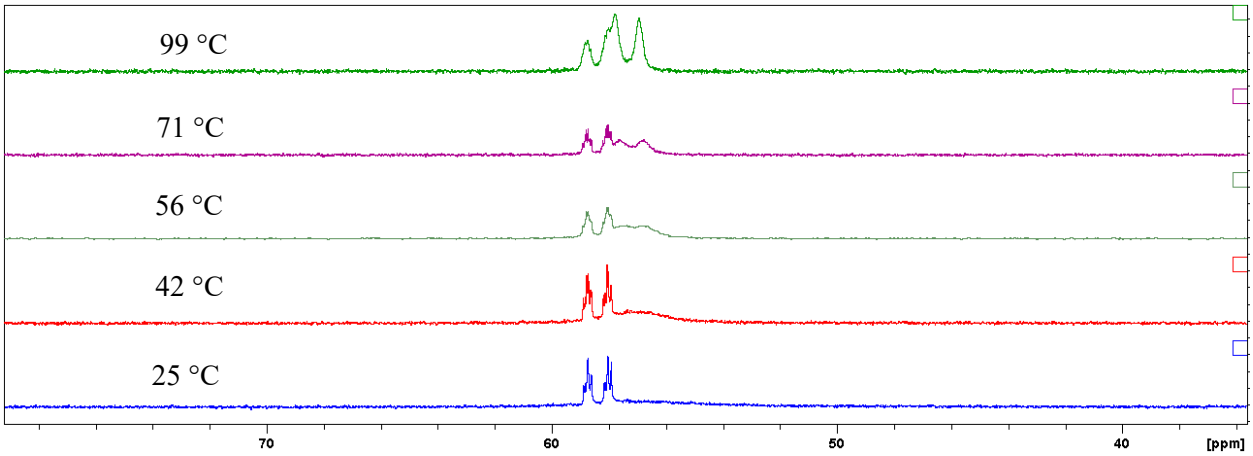

Figure S46. High temperature VT $^{31}P\{^{1}H\}$ NMR spectra of **2-H** (162 MHz) in toluene- d_8. At room temperature, the only visible phosphorus signal corresponds to the phosphine *trans* to the hydride ligand (labeled as P_2 in main text). The other two phosphorus nuclei are not visible at room temperature because they are near coalescence (labeled as P_1 and P_3 in main text). At higher temperatures the two phosphines *cis* to the hydride are equivalent and appear as a doublet, corresponding to both $P_{1,3}$.

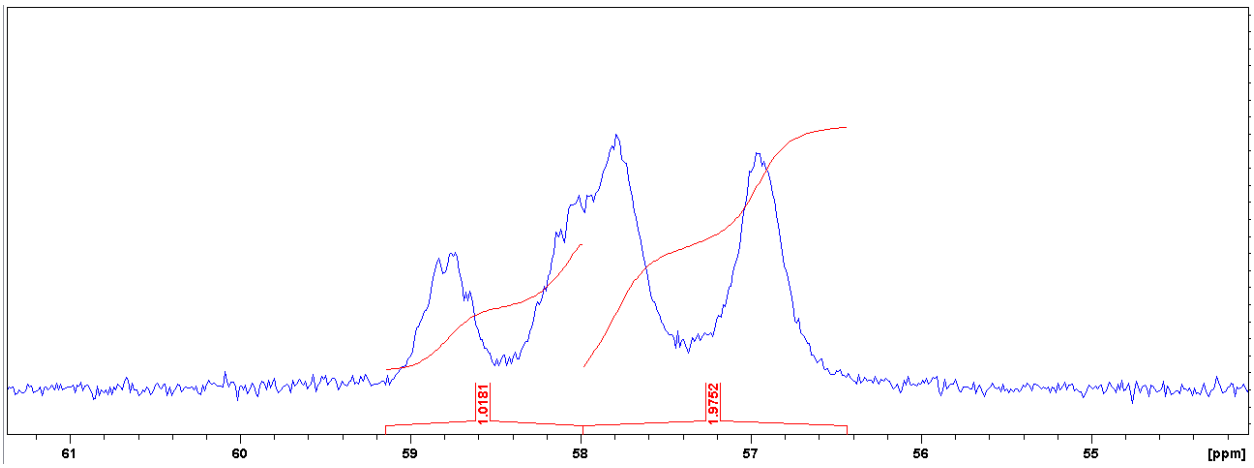

Figure S47. $^{31}P\{^{1}H\}$ NMR spectrum of **2-H** (162 MHz) in toluene- d_8 at 97°C.

Table S1. Calculation of approximate rate constants and energy barriers for the fluxional processes that equilibrate P_1 and P_3 for all complexes.

	1-Cl	**2-Cl**	**1-CH3**	**2-CH3**	**1-H**	**2-H**
T_c (K)	359	345	>370	>370	265	279
Δ (Hz)	2905.7	3338.9	3493.7	3749.6	2562.8	2482.4
J (Hz)	317	325	314	317	265	273
k_c (s^{-1})	6681	7625	7947	8506	5873	5711
$\Delta G^{\ddagger}$ (kcal/mol)	14.9	14.2	>15.2	>15.2	10.9	11.5

where $k_c = (\pi/\sqrt{2}) \times (\sqrt{\Delta\nu^2 + 6J^2})$[1] for a coupled system and Eyring relationship, $\Delta G^{\ddagger} = RT_c[23.76 + ln(T_c/k_c)$.

References

1. D. Kost; E. H. Carlson; M. Raban. *J. Chem. Soc. D*, **1971**, *13*, 656.